Anti-Islanding Protection of PV-based Microgrids Consisting of PHEVs using SVMs

Baghaee, H. R.; Mlakić, D.; Nikolovski, S.; Dragičević, Tomislav

Published in:
IEEE Transactions on Smart Grid

DOI (link to publication from Publisher):
10.1109/TSG.2019.2924290

Publication date:
2020

Document Version
Accepted author manuscript, peer reviewed version

Anti-Islanding Protection of PV-based Microgrids Consisting of PHEVs using SVMs

Hamid Reza Baghaee, *Member, IEEE,* Dragan Mlakić, *Student Member, IEEE,* Srete Nikolovski *Senior Member, IEEE,* and Tomislav Dragičević, *Senior Member, IEEE,*

***Abstract*—The cheap and reliable primal energy source for BESS refueling necessitates a special attention for combining RERs with PHEV charging stations in microgrids. Rapid charging is an operation mode of PHEV for drivers which demands fast recharging of BESSs of the electric cars. This charging mode manifests as low impedance short circuit at DC side, making power transient on power grid side. This paper presents a new anti-islanding protection scheme for LV VSC-based microgrids by exploiting SVMs. The proposed anti-islanding protection method exploits powerful classification capability of SVMs. The sensor monitors seven inputs measured at the PCC, namely RMS value of voltage and current (RMS_V, RMS_I), THD of voltage and current (THD_V, THD_I), frequency (f), and also active and reactive powers (P, Q). This approach is based on passive monitoring and therefore, it does not affect the PQ. In order to cover as many situations as possible, minimize false tripping and remain selective, training and detection procedures are simply introduced. Based on the presented sampling method and input model, the proposed method is tested under different conditions such as PHEV rapid charging, additional load change and multiple DGs at the same PCC. Simulations based on the model and parameters of a real-life practical PV power plant are performed in MATLAB/Simulink environment, and several tests are executed based on different scenarios and compared with previously-reported techniques, this analysis proved the effectiveness, authenticity, selectivity, accuracy and precision of the proposed method with allowable impact on PQ according to UL1741 standard, and its superiority over other methods.**

***Index Terms*—Anti-islanding protection, distributed generation, microgrid, photovoltaic, plug-in hybrid electric vehicles, power quality, support vector machine.**

H.R. Baghaee is with the Department of Electrical Engineering, Amirkabir university of Technology, Tehran, Iran, e-mail: (hrbaghaee@aut.ac.ir).

D. Mlakić is with the Department of Measurement and Network Management in Electrical Energy Systems, Distribution Area, Centar", JP Elektroprivreda HZ HB" d.d, Mostar, Mostar, Bosnia and Herzegovina (e-mail: dragan.mlakic@ephzhb.ba).

Srete Nikolovski is with the Power Engineering Department, Faculty of Electrical Engineering, Computer science and Information Technology, University of Osijek, Osijek, Croatia (e-mail: srete.nikolovski@ferit.hr)

T. Dragičević is with the Department of Energy Technology Power Electronic Systems, Faculty of Engineering and Science, Aalborg University, Aalborg 9220, Denmark (e-mail: tdr@et.aau.dk).

$Corresponding Author$: Srete Nikolovski (srete.nikolovski@ferit.hr)

Manuscript received July XX, 2018; revised August XX, 2018.

NOMENCLATURE

Abbreviations/Acronyms

AC	Alternating Current
ADF	Active Frequency Drift
ADN	Active Distribution Networks
AI	Artificial Intelligence
ANFIS	Adaptive Neuro-Fuzzy Inference System
ANN	Artificial Neural Networks
APS	Automatic Phase Shift
BESS	Battery energy storage system
CB	Circuit Breaker
DC	Direct Current
DG	Distributed Generation
DER	Distributed Energy Resources
DN	Distribution Network
DSP	Digital Signal Processing
DT	Detection Time
ESS	Energy Storage System
EV	Electric Vehicles
FC	Fuel Cell
FL	Fuzzy Logic
FDZ	Fault Detection Zone
FIFO	First In First Out
FPGA	Field Programmable Gate Array
HMI	Human Machine Interface
IED	Intelligent Electronic Device
IGBT	Insulated Gate Bipolar Transistor
LV	Low-Voltage
ML	Machine Learning
MPPT	Maximum Power Point Tracking
NDZ	Non-Detection Zone
PCC	Point of Common Coupling
PFNN	Probabilistic Fuzzy Neural Network
PHEV	Plug-in hybrid electric vehicles
PQ	Power Quality
PV	Photovoltaic
PWM	Pulse Width Modulation
QF	Quality Factor
RER	Renewable Energy Resources
RMS	Root-Mean-Square
ROCPAD	Rate of Change of Phase Angle Difference
SFS	Sandia Frequency Shift
SLD	Single Line Diagram
SMFS	Sliding Mode Frequency Shift
SVM	Support Vector Machine
THD	Total Harmonic Distortion
VSC	Voltage-Sourced Converter
WG	Wind Generation

Variable/Parameter	
f	System frequency
P	Active power
Q	Reactive Power
RMS_I	RMS value of current
RMS_V	RMS value of voltage
THD_I	THD of current
THD_V	THD of voltage
P_{Load}, Q_{Load}	Active/Reactive Components of Energy Consumed by RLC Load in Synchronized Mode of DG and DN
P_{Charge}, Q_{Charge}	Active/Reactive Powers of Load During Charging Scenario
P_{PV}, Q_{PV}	Active/Reactive Powers Generated by PV Unit Delivered at the Output of VSC
$\Delta\ P$, $\Delta\ Q$	Active and Reactive Energy Delivered to DN
T_s	The Integration Period
n	Number of the observed parameters
$y^{'}$	Kernel binary classifier of the predicted label for $x^{'}$
$x^{'}$	Kernel function that makes segregation between pair of inputs x
N	Kernel dimension and sum ranges over all of them with y_i
ω_i	Weight for training samples
$sign$	A function determining sign of function y_0 which may be positive or negative
x	Input vector
$x^{'}$	Measured data stack for classification
γ	Kernel scale parameter
ω	Normal vector orthogonal on hyperplane
$\Re^n$	Euclidean space
Q_f	Quality factor
U_n	Nominal distribution network voltage
$P_{installed}$	Installed power capacity of DG
I_{acu}	Index rate for accuracy
N_M	Number of active and passive methods used in this paper
I_{NDZ}	Index rate for NDZ
N_{act}	Number of active techniques used in method
A_M	Constant of active techniques
N_{pas}	Number of passive techniques used here
P_M	Constant of passive techniques

I. Introduction

ANTI -islanding protection method implemented into the inverter is one of key factors in PQ of VSC-based LV distribution networks (DNs) and microgrids including DERs and ESSs (in this paper, a PV power plant located in Jajce, Bosnia and Herzegovina (Fig. 1)). According to IEEE Std. 1547 [1], DG shall detect the situation for any possible islanding conditions and cease to energize the area within 2 sec. for small voltage and frequency signal variations. When islanding occurs, the main concerns are the potential danger for human safety, electrical equipment fault possibility, and the consequent PQ issues regarding DG autonomous operation [2].

Generally, the islanding detection strategies can be classified into local and remote (communication-based) categories. Communication-based islanding detection techniques cover the most of NDZs using communication technologies, by confirming distribution network CB is out of state to prevent islanding [3]. The cost of equipment and moreover, reconfiguration of settings every time when new component is added or taken from grid, are the major drawbacks of these methods. The local islanding detection methods work based on local measurement of grid signals and include active, passive and hybrid techniques. Relying on latter approach, we introduce a new class of local islanding detection strategies based on AI and ML in our past and future works [4]. Recently, ML algorithms have been used for analyzing grid signals.

The methods based on active entanglement and passive monitoring are localized algorithms for recognizing islanding mode which are working based on tracking and/or changing particular parameters of DN such as voltage [3], reactive power [5], frequency [6]. By injecting the disturbances into DN at the PCC and tracking down the response of DN, the active methods tend to make the most negative impact to PQ and thus they have. So they have limited applications. The active methods have much smaller NDZ than the passive techniques that only monitor a particular parameter. However, some methods tend to become more optimized by minimizing NDZ [7], [8]. At the first look, this may appear as a disadvantage. However, there are some active methods (like [9]) that are actually optimized in terms of more than one parameter (e.g. [9] that is optimized in both terms of NDZ and FDZ). There are recently published works e.g. [9], [10], where active methods have been efficiently used for anti-islanding protection of DERs under high-penetration levels and weak grid conditions to address some of the mentioned concerns. Some of the most popular active methods are-high frequency signal injection [8], [11], AFD [12], improved AFD [13], SFS) [6], [7], [14], [15], fuzzy SFS [16], APS [17], SMFS [18], [19], impedance measurement [20], singular and dual harmonic current injections [21]–[23], high frequency signal injection [24]–[29], output power variations [30], reactive power variation and control [31]–[34], and active current disturbance [35]. Other, worth noted active anti-islanding schemes are presented in [32], [36], [37].

Passive-based methods track the trends of some parameters in the PCC cyclically and then compare the sampled values with a predefined threshold. Depending on the quantity and quality of the followed parameter, these methods not only tend

to have the biggest NDZ, but also minimal impact to PQ. Some of the most popular passive techniques are under/over voltage, under/over frequency [38], rate of change of frequency [39], [40], phase jump detection [41], rate of change of frequency with power [42], rate of change of power with THD [43], voltage unbalance and THD of current signal [44], voltage and power factor change [45], energy mismatch for the harmonics etc. [46], ROCPAD [47], rate of change of reactive power [2], and rate of change of independence [8]. These methods do not have any negative impact on the grid operation, but they are characterized by larger NDZ than active methods. To decrease NDZ of the passive methods, advanced signal processing tools such as Duffing oscillations [48], wavelet transforms and S-Transform [49], are exploited.

Hybrid methods combine new groups of anti-islanding protection methodologies to take the advantage and leave out the shortages of passive and active methods into one localized islanding protection scheme [11], [50]. At the first look, it seems that the NDZ is mostly covered by active techniques, but new obstacles arrive when more parameters are involved by combining them with passive techniques. The PQ problems may be raised including but not limited to frequency deviation, voltage fluctuation, harmonics and power factor instability.

The more updated category of local islanding detection methods are smart techniques based on AI techniques. Different methods have been reported based on ANNs [5], ANFIS [4], [6], [8], or FL [51], relevance vector machine [52], PFNN [53], logistic regression [54], and some other combined with active and passive techniques [16]. The PHEV charging can be differentiated by some tools like ANNs, but in this paper, we propose a complete algorithm based on one AI technique for islanding detection, and its discrimination with PHEV rapid charging. It can be easily retrained and maintained.

This paper presents two new basic contributions combined into one unified framework: 1) anti-islanding protection based on SVMs, and 2) participation of PHEV charging stations in LV-DN which can affect the performance of the anti-islanding protection scheme (Fig. 2). The basic contribution of this paper is anti-islanding protection of microgrid using SVMs. However, the second item of the contribution is not dealing only with investigation of the effect of the PHEV on micorigrd. The second contribution is the successful operation of the proposed anti-islanding strategy or discrimination of unplanned islanding with rapid charging of PHEV.

The basic motivation of this research beside interconnection of DG units into the grid, is investigation of the effect of PHEV rapid charging on LV-DN as a huge load with small resistance which can make an unexpected transient in microgrid. In this paper, the recognition capability of SVM (which is one of the newest and most prominent ML-based classification techniques) is exploited to make the presented anti-islanding protection method attractive for LV-DNs and microgrids. More importantly, the idea of the paper has enough generality to be applied for all generic microgrids. We evaluated the performance of the proposed strategy for several scenarios such as UL1741 standard test conditions, additional load injection, multiple DG cases, and PHEV charging. We also, compared the proposed method with several reported techniques to prove its efficiency, authenticity, accuracy, and operation speed. By reviewing Section IV (Simulation results) we can understand that the proposed method has enough level of generality to be applied for all kinds of generic microgrids. The database which has been used for the training algorithm, has been gathered based on experimental measurement (using IED shown in Fig. 3) in a real-life PV plant located in Jajce, Bosnia and Herzegovina (Fig. 1). Moreover, this paper introduces a new approach for pre-processing of the input data set into an AI/ML-based classification algorithm used for anti-islanding protection in a microgrid including PHEV. In fact, SVM performs as a dual-functional classifier to classify islanding and grid-connected modes, and discriminate them with rapid charging of situation PHEV. To the best of authors' knowledge, this paper is the pioneer for proposing SVM as a dual-functional classifier to realize these objectives. The cross-validation for over-fitting protection is included by means of a default Gaussian function.

The remainder of this paper is organized to cover the mentioned theme and realize design objectives as follows: Section II elaborates on description of the study system and sampling model for acquiring data for data stack which is the input for SVM training and anomaly classification. Section III presents proposed islanding detection method. Verification of the performance and viability of the proposed anti-islanding protection scheme, based on offline digital time-domain simulations and comparison with other reported techniques are presented in section IV. Finally, conclusions are stated in section V.

II. Study System

This section presents the sampling model used to feed algorithms with new data required for prediction procedure. It is known that when samples are enough small in time scale, the data processing and analysis are conducted much more comfortable to be achieved. These samples are essential bases for right conclusion about the analyzed issues.

Fig. 2 shows the study system including a 20 kW PV unit as a DG, an external RLC impedance for voltage and current adjustment in a 0.4 kV LV-DN, a parallel RLC load, and a BESS with 129 Ah capacity. The roof fixed PV acts as a constant current source with 300 V DC voltage at the inverter input. The 1Soltech 1STH-215-P PV strings with specifications given in Table II are set at the MPPT mode with MPPT characteristics discussed in [55], for solar irradiance of 1000 kW/m^2 and outside panel temperature of 25 ^oC. The DC/AC inverter is modeled as a 6 pulses IGBT-based VSC, with PWM generator, that takes the reference signals from frequency and amplitude controllers. The DG unit is connected to LV-DN at the PCC through CB. A RL impedance is used to model the internal impedance of DN power source. When islanding is detected at the PCC, the CB isolates the DG unit from DN. The ESS is modeled based on information provided in Table I which have been extracted almost from [56]. From Fig. 2, the energy consumed by the load and ESS is the sum

(a) (b) (c) (d) (e) (f)

Fig. 1. Elements of PV power Plant and connection to DN: (a) PV panels on rooftop with installed power of 23.8 kW, (b) AC cabinet on concrete pillar with measurement and protection equipment, (c) AC and DC cabinet and inverters 2×10 kW, (d) smart meter with line breaker, (e) smart UPS, and (f) line breaker.

TABLE I
CHARGING STATION PARAMETERS [56]

Parameters	Values
Input Parameters	
Grid configuration	3 phase
Grid voltage	0.4 kV
Grid frequency	50 Hz
ESS charging current	100 A
P_{ESS}	200 kW
V_{batt}	380 V
L_{batt}	2 mH
R_{batt}	0.0175 Ω
ESS capacity	10 kWh
SoC	50%
ESS activation time	0.1 sec.
QF	5
Output Parameters (Charging mode)	
$P_{ESS-charging}$	1.2 MW
L_{rect}	0.48 mH
R_{on}	0.01 Ω

of the energy delivered from the grid and the energy generated by DG source is given by:

$$P_{Load} + jQ_{Load} + P_{Charge} + jQ_{Charge} = P_{PV} + jQ_{PV} + \Delta P + \Delta Q \quad (1)$$

Note that P_{Charge} and Q_{Charge} are different in two scenarios: charging of ESS and rapid charging of PHEV. There are a huge difference between the values of power in these two cases. In this paper, we propose a new strategy based on SVM for anti-islanding protection in a microgrid including PV unit and PHEV. We study the operation of the microgird based on the experimental measurement of some signals practically, and then, simulate the proposed islanding detection strategy not only for islanding detection, but also for discrimination of islanding phenomenon with rapid charging of PHEV. The microgird can operate in islanding and grid-connected modes. But, our proposed strategy aims to detect unintentional islanding phenomenon. When microgrid is connected to the main grid, it looses its micro part if considering bidirectionality of power. That is due to ESS nature of constant motivation to be 100% SOC. The energy is unidirectional from main grid to PHEV microgrid. Scheme of PHEV recharging station is simplified due to theme of this paper "Anti-Islanding Protection", but it executes its part.

In this paper, samples are acquired by custom-made improvised electronic device (IED) in role of a network analyzer which takes role of voltage and current measurement device. Fig. 3 shows the equipment for on-site measurement of voltage and current in PCC for PV plant and DN. The measurement device, shown in Fig. 3, is a network meter including a current measurement transformers model No. ENTES ENT.B 75/5 A in combination with TA12-100 5A, voltage transformer model No. ZMPT101B, and Arduino UNO board R3. The software for data storage is programmed using Java programming language. The details of IED have been provided in [4], [55], [57]. Reduction of the DT and NDZ are the most important goals of current research to achieve a high level of accuracy

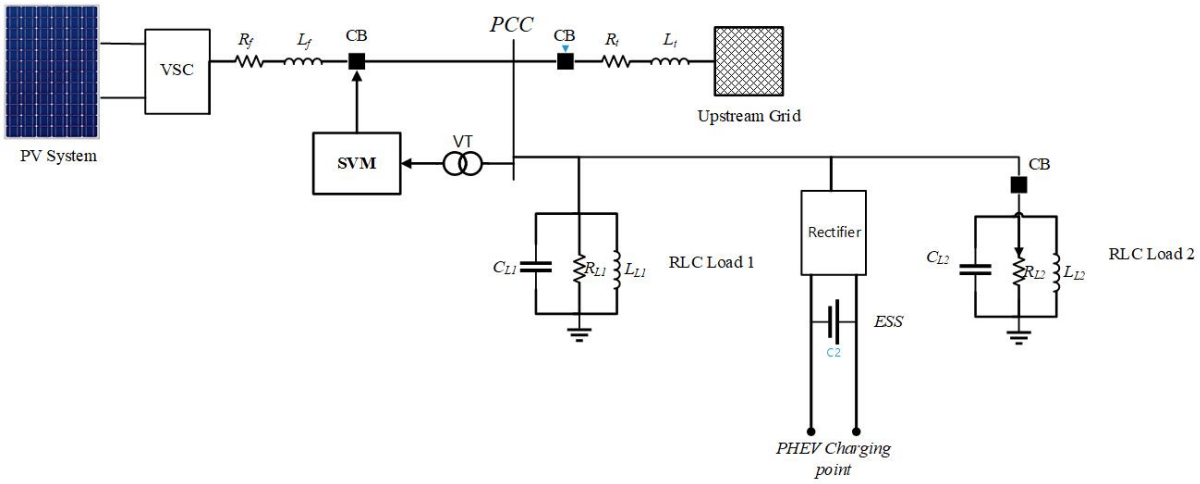

Fig. 2. Single line diagram of test system based on a real-life practical microgrid.

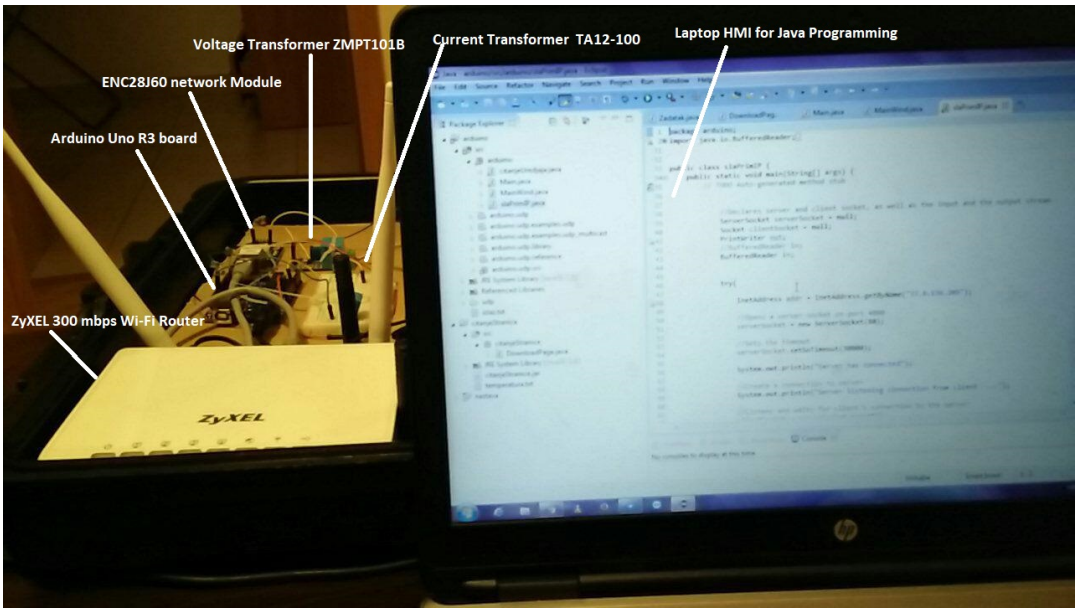

Fig. 3. Details of IED assembled for on-site measurement at PCC.

TABLE II
1SOLTECH PV PANEL SPECIFICATION

Solar Panel Specifications	
PV Model at STC	1Soltech STH-215-P
Standard test conditions	1000 W/m2, 25 C
Maximum voltage	29.0 V
Maximum current	7.35 A
Maximum power	213.15 W
Number of cells in series	60
Short circuit current	7.84 A
Open circuit voltage	36.3 V

A. PHEV Charging Station

Fig. 4 shows the block diagram of the recharging strategy and voltage control model that has been proposed by [56], [58]. A bidirectional buck-boost converter is used as the interface between the EV battery and the battery of the charger and the control scheme of Fig. 4 is applied to this converter. In fact, this is controller for battery charging and voltage stability in battery and also overcharging controller for battery bank. This recharging controller takes the grid effective voltage as its input for recharging controller. In this way, the amplitude of the voltage will stay same as the case of rapid charging. The parameters of BESS and rectifier are taken from [56], [58] and presented in Tables III and IV, respectively. It should be noted that some of these parameters are custom taken from authors of paper according to the testing model.

The BESS is implemented in role of charging station ESS so that it can accumulate the energy for PHEV customer. In this way, the energy for rapid charging is ready for reclaiming with minimal load on grid at the moment of charging. The rectifier is in charge of adapting distribution LV grid and DC side of the BESS. In case that we have no PHEV charging, the rectifier recharges the BESS and supplies a part of load during charging scenario. The active impedance of PHEV in charging scenario

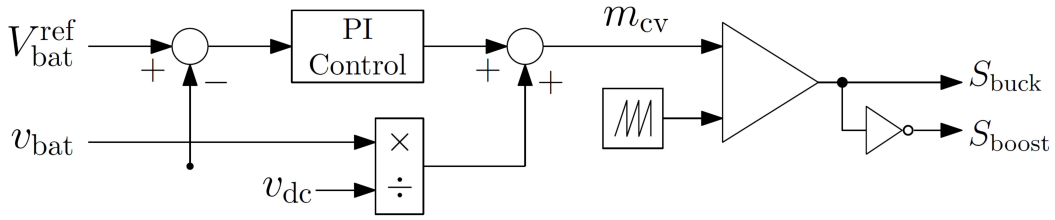

Fig. 4. Constant voltage strategy recharging control [56].

TABLE III
PARAMETERS OF BESS IN CHARGING STATION [56], [58].

Parameter	Value
Nominal voltage [V]	100
Rated capacity [Ah]	129
SOC [%]	50
Battery response time [sec.]	0.2
Nominal discharge current [A]	5608
Internal resistance [Ω]	0.007

TABLE IV
PARAMETERS OF THE RECTIFIER [56], [58].

Parameter	Value
Resistance [Ω]	0.001
Inductance [H]	0
Nominal line voltage [RMS_V]	390
Source frequency [Hz]	50
DC bus capacitance [F]	0.0075

is 0.01 Ω. On account of the fact that a very small resistance of DC grid affects the LV-DN to be seemed as almost short circuit, the islanding detection strategy shall recognize the rapid charging of PHEV as non-islanding scenario and give no signal to protection relay and CB considering the nature of the event. The complete model is depicted in Fig. 2 which has PHEV charging station. Note that representation of electrical vehicle is not presented on scheme on Fig. 2 because rapid charging is simulated via small inner resistance of vehicle battery bank system. Therefore, vehicle is presented as simulation part only as rapid charging part. In this paper, PHEV is not the primary consideration of authors and therefore, any strategy of vehicle charging service, scheduling charging, rapid or regular charging, pricing, energy cost, PHEV power management, and loses in charging process are not discussed in paper. Islanding during charging is considered as a scenario in Section IV. Note that in this paper, we will not investigate the optimal power management of microgrid including PV ad PHEV. We just investigate the effect of the PHEV on the performance of the proposed anti-islanding strategy.

Fast charging algorithm for the battery can be represented by the fast current pulse, which is followed by a continuous reduction of the charging current as dictated by the battery charging algorithm. Since the most meaningful part for our detection strategy is the initial current pulse, this is the only part that we have modeled. It should also be noted that modeling the whole charging procedure would not provide any additional advantages. Therefore, we decided to avoid it. Also, charging algorithm for PHEV is explained in [59].

The next important issue is the definition of simulation integration time step. As proposed in [56], to achieve good results, integration period should have at least 100 samples in the period of fast frequency of inverter switching. In this paper, f = 10000 Hz is considered as the fastest frequency for inverter switching frequency. Thus, the integration period is calculated as:

$$T_s = \frac{1sec.}{10000 \times 100} = 1\mu sec. \tag{2}$$

B. Sampling Model and Data Pre-processing

The required samples for SVM training are acquired by experimental measurement device at the PCC of a real-life practical PV plant (Fig. 1). The measurement device, shown in Fig. 3, is a network meter including a current measurement transformers model No. ENTES ENT.B 75/5 A in combination with TA12-100 5A, voltage transformer model No. ZMPT101B, and Arduino UNO board R3. In this paper, samples are acquired by using a custom-made IED as a network analyzer which plays the role of voltage and current measurement devices. This figure shows the equipment for on-site measurement of voltage and current in the PCC of PV and include a brief closed view of IED with its components such as Wi-Fi modem and router, HMI in laptop, Arduino UNO R3 motherboard, preferal sensors, and connecting wires. The software for data storage is programmed using Java programming language. In hardware, we used standard PC RAM memory based on DDR4-2133 modules for data storage software in stack is standard Java variable "*double*" and then, processed further to MATLAB/Simulink via software port. The details of IED have been provided in [57]. The rate of sampling defines the quality of classification of the input data which further defines the effectiveness of the proposed method. Reducing the DT and NDZ are the most important goals of current research as well as achieving high accuracy, assuming that the sampling time is chosen considering anomaly signal behavior, where all 7 signals behave according to grid conditions. The signals are sampled in time window of 5 msec. where this behavior is segmented in 8 samples.

There are 8 samples and whole signal data stack has 40 msec. duration. Therefore, the signal noises are ignored in case they are shorter than 5 msec. and are taken into account as signal behavior if they last between 5 to 40 msec. The described sampling approach is depicted in Fig. 5. The sampling time, and number of samples in one data stack increases the

TABLE V
SIGNAL AND SAMPLING DETAILS

Signal	Sampling time (sec.)	Amount of Samples	Data Stack Sample time (sec.)	Data stack frequency (Hz)
RMS_U, RMS_I, THD_U, THD_I, f, P_G, P_G	0.005	8	0.04	200

selectiveness of the proposed sampling method. Consequently, with more selectiveness, the growing NDZ comes. Reduction of NDZ requires involving different signals affected by islanding state. When selectiveness is high, the method tends to loose generalization over the input data which leads to avoid recognizing islanding operating mode of DG unit. To minimize NDZ and maximize accuracy, an optimal relation (trade-off) should be made between selectiveness and generalization. In this favor, high number of testing samples are required. This paper proposes a novel method holds on passive nature of islanding detection by monitoring seven parameters of DN, each responsible for one energy quality parameter. These signals are RMS_U, RMS_I, THD_U, THD_I, f, P_G, and Q_G. These seven signals cover the most of islanding affected anomalies and therefore, they all are important to accurate detect islanding of DG unit. It is very hard to detect the islanding phenomenon when there is no RMS_V change in islanding scenario, so there should be more signals included in detection process. Also, there is a same story with other signals such as THD_V and THD_I and therefore, more signals are included intending to achieve to the goal of minimizing NDZ and maximizing accuracy in islanding detection and its discrimination with rapid charging of PHEV. With all seven signals involved in islanding detection, the proposed method minimizes the NDZ. The sampling data sequence of 8 samples is stored in data stack with operating regime of FIFO. Every new sample is placed on top of data stack and oldest one is pushed out of stack, keeping data stack fresh and up to date for timely detection. The data stack is the input data block for training of SVM algorithm for all seven parameters, and further for discriminating islanding and PHEV rapid charging conditions. The details of signals, sampling rate, and sampling time are presented in Fig. 5 and Table V. Fig. 5 depicts the sampling rate where each signal is sampled 4 times in one waveform period of 20 msec. Every 5 msec., one sample is taken for all 7 signals and stored in signal data stack for input data packaging for SVM controller.

For the cost of implementation of the proposed strategy, it should be noted that the proposed method does ot necessitate any extra measuring device for the system ad all required signal can be measured by using the commercially-available meters that are usually installed on the microgrid PCCs. Also, the SVM blocks can be easily implemented on low-cost high-performance FPGA or DSP devices.

III. PROPOSED ISLANDING DETECTION AND GRID FAULT DETECTION STRATEGIES

SVM is a discriminating classifier which is formally defined by a separating hyperplane. In other words, given a labeled training data (supervised learning), the algorithm outputs an optimal hyperplane which categorizes new examples. In a two-dimensional space, this hyperplane is a line dividing a plane into two parts where each class lays in either side. This can be very much complex goal to achieve data needed to discriminated into two sets [60].

A. Basic Concepts

The proposed method is heavily based on the principle that "*Minimizing of NDZ require involving more signals in detection procedure with their deviation during occurrence of anomaly*". These signals are frequency (f), active power (p), reactive power (Q), RMS value of current (RMS_I), RMS value of voltage (RMS_V), THD of curent (THD_I), and THD of voltage (THD_V).

Whole system for discrimination and detection is assembled by using previously-mentioned SVM-based islanding detection module of the proposed algorithms. The detection, classification and prediction functions of SVM are combined into one "if" loop for final output. These SVM algorithms for particular signals automatically predict based on input data stack provided by IED-network analyzer recorded data. Information for all signals is solely based on two measured values namely voltage on all three LV phases and current on all three phases.

For calculating the f, since IED sends data constantly to Java software, the software clock is set up to receive data by 1 msec. which give us the access to calculate the current. The data taken from IED to Java program are used for signal calculation according to the below formulas for respected signal. It is taken for the physical model of system simulated in Matlab/Simulink software environment. All recorded data are used for accurate modeling as much as possible in software tool. After that, the model is used for proposed method training and testing. Every 1 msec., one measured point in the voltage and current signals are transmitted. The input data stack for SVM classification needs a 5 msec. sample. Therefore, in one cycle of the waveform, we have 4 samples in 20 msec. Every sample block has 5 samples in a 1 msec. time window. If we compare the peak values of current and voltage, we will find out how much current delays (lags) after voltage or vice versa. That gives us access to divide impedance into inductive and resistivity component. Every signal is served by one specific SVM module for its related signal. The pre-processing of the sampled signal is done in the form of FIFO stack and packed into input data which is the input for SVM module. Based on the input data deck, the SVM module produces a predicted classification output for a given deck. Fig. 6 depicts the sampling architecture for one of seven signals with SVM at the end of the block.

The entire of the proposed anti-islanding protection algorithm is illustrated in Fig. 7.

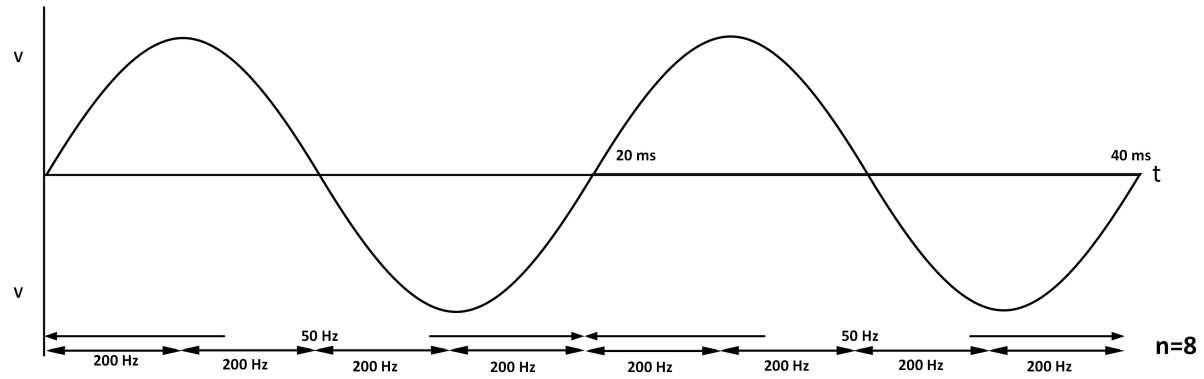

Fig. 5. The proposed signal sampling method affected by the grid states.

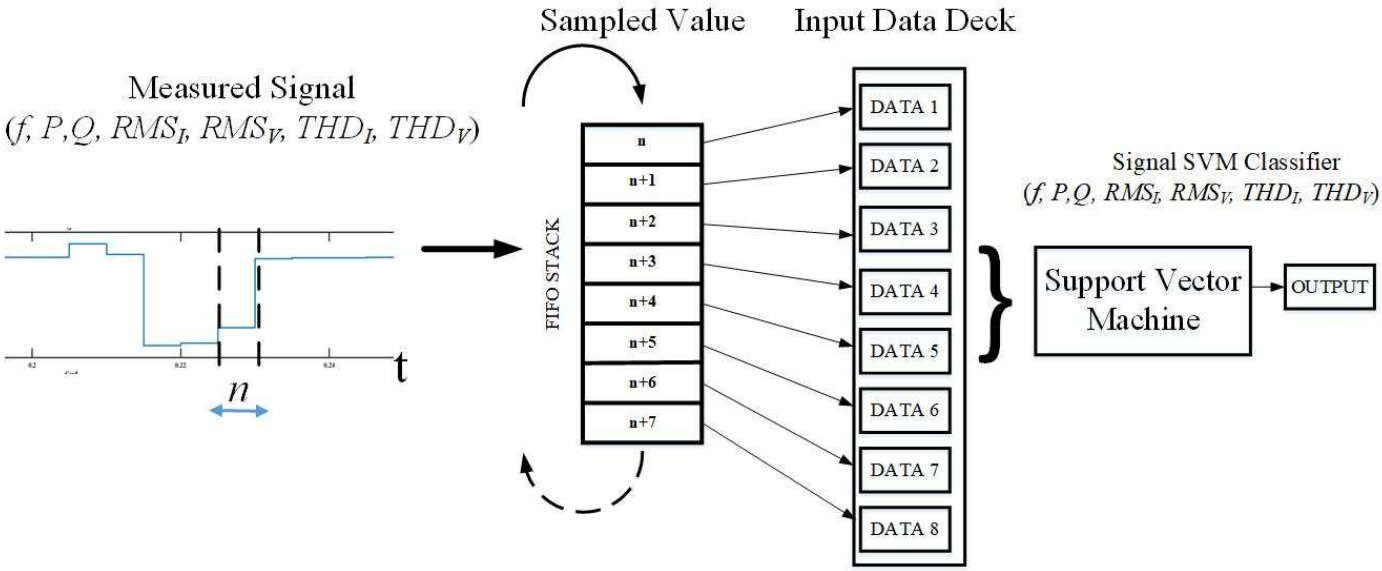

Fig. 6. The proposed sampling architecture for a specific signal.

B. SVM-based Islanding Detection

SVM is essentially a supervised machine learning algorithm which can be used for many different challenges involving classification or regression of a given data set. Due to its nature, SVM is almost used for classification problems so that one data set differs from another one using some hyperplane. Visual and logical representation of SVM is plot of each data item as a point in n-dimensional space with the value of each feature fits the value of a particular coordinate in n-space. Then, the classification is performed by finding the hyperplane that differentiate two classes to given satisfaction level (Fig. 8)

In this paper, the differential classes are two situations: islanding mode happened or not happened in DN. The block used for SVM training contains 8 values, which means that SVM kernel level is 8, and further means that the designed SVM-based algorithm performs classification in a 8-dimensional space. The hyperplane in $\Re^n$ is an n-1 dimensional subspace. Consistent to this idea, it can be concluded that the current value of n is 8 and the hyperplane for it is a 7-dimensional subspace. Also another priority task for successfully classify two sets of data is margin. The reason for choosing large margins is to avoid high probability of miss-classification of input data. however, it will not result in FDZ at all and as we show in the simulation results (Section IV), the NDZ is minimized compared to the most of the well-known reported AI-based techniques, keeping the accuracy at the highest possible level i.e. 100%. Choosing large margin ensures clear and visible distinction between input data, while with large margin, when training data allows, there is a clear boundary between one data set and other one so that we have good discrimination between those two goals for effective SVM method. Large margin helps the proposed method by preventing mis-classification of input data. Sole kernel is not enough for that role because it does not gives any gap between two data sets and therefore does not provide clear security from mis-classification.

Prior to the margin definition, the SVM first chooses right hyperplane. The right hyperplane indirectly defines the margin. Choosing right kernel needs to be done respectfully to all input signals namely RMS_U, RMS_I, THD_U, THD_I, f, P_G, and Q_G. Even kernel level is 8, there might be need to do kernel

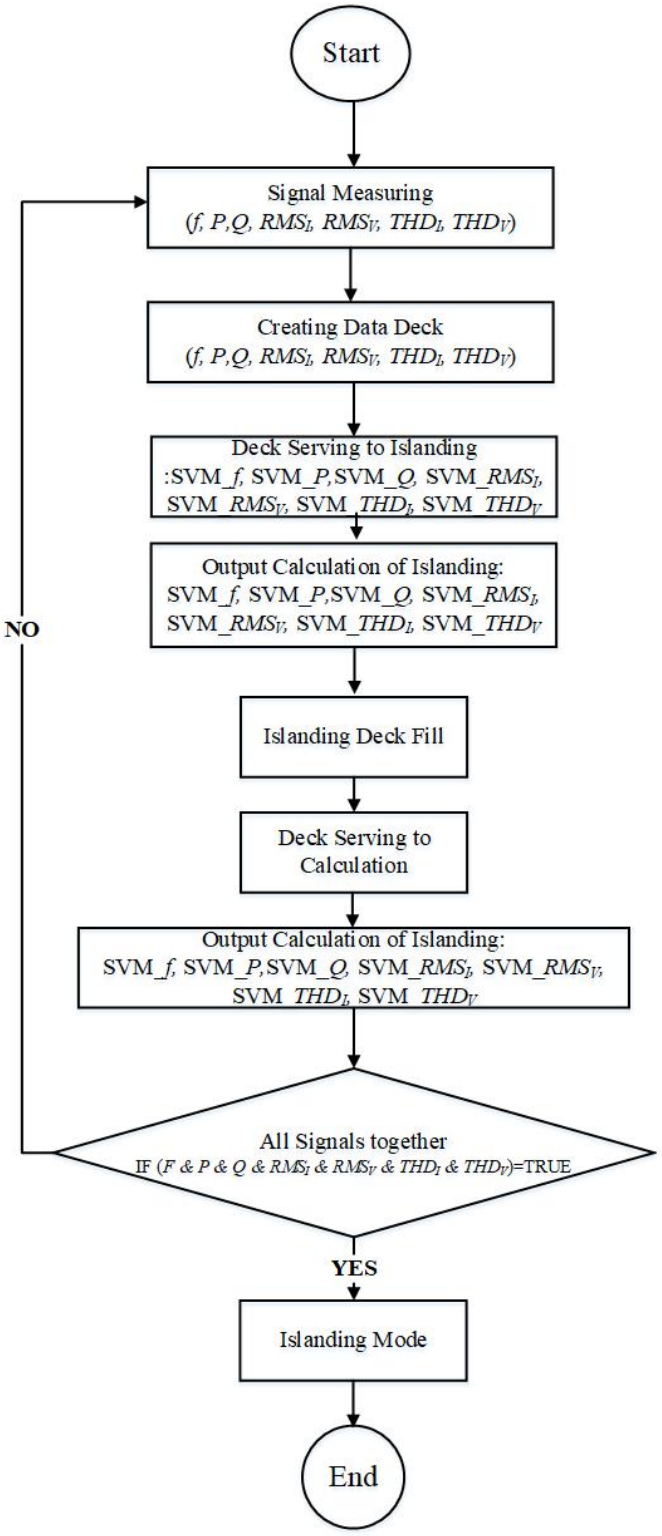

Fig. 7. Overview and block diagram of the proposed method.

trick which is a sub-task to select right hyperplane. The kernel is defined as [60]:

$$y^{'} = sign(\sum_{i=1}^{N} \omega_i y_i k(x_i, x^{'})) \quad (3)$$

where, $k : X \rightarrow x$, In this paper, N is 8 if the expression

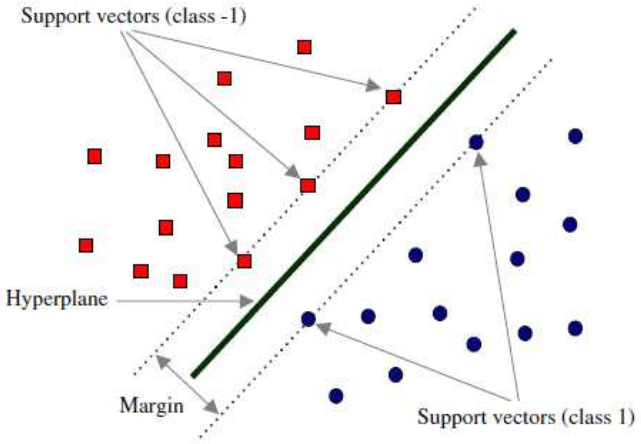

Fig. 8. General representation of classification hyperplane in SVM algorithm.

(3) satisfies the classification based on input data. The input data set is shown in Figs. 9, and 10. All of the mentioned figures present the same input signal and the only difference is dimension of input string. While it is impossible to present up to dimension 8, Fig. 9 shows the input data string up to its third dimension.

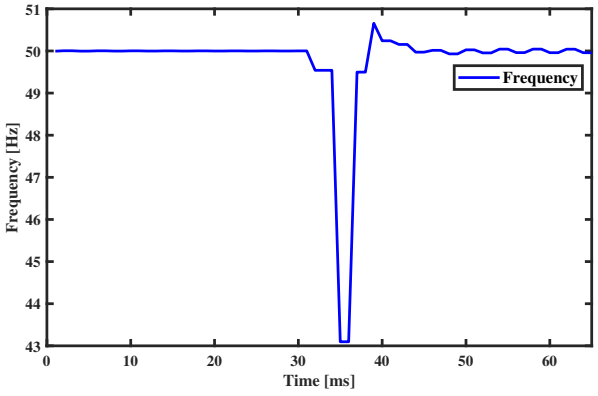

Fig. 9. Frequency input stream's one dimension input data.

In Figs. 9 and 10, the data is presented and limited to the frequency. The same illustration can be done for all other remained six signals. From these figures, the data positioning is clear: most of the normal operation states of the grid is clustered around 50 Hz on all three dimensions. Therefore, segregation between normal and islanding distribution grid operation mode is submitted to global maximum of 50 Hz. The best description with Gaussian function and with the arguments suitable for frequency case is chosen as [60]:

$$K(x, x^{'}) = e^{(-\gamma(\|x - x^{'}\|)^2)} \quad (4)$$

where, $x \in X$:50, 50, 50, 50, 50, 50, 50 is input vector of dimension 8, γ is used to divide all elements in kernel Gram matrix. Determination of γ is left to the software since it is done by random number generation machine but involving

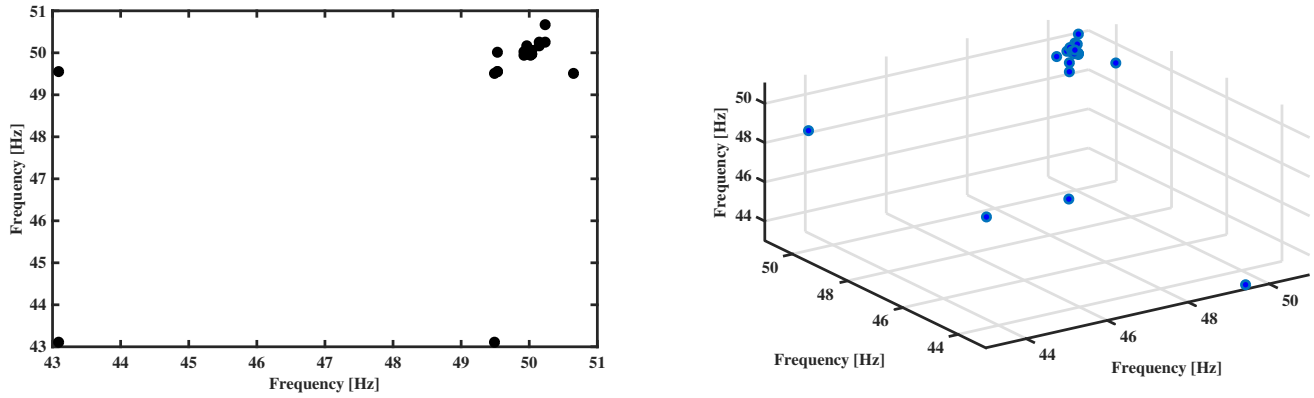

(a) (b)

Fig. 10. The input data string: (a) 2D input data, and (b) 3D input data.

optimal solution based on training samples. The hyperplane that can be described according to Fig. 8 is given by:

$$\overrightarrow{\omega}\,\overrightarrow{x} - b = 0 \tag{5}$$

where, ω is a unit vector for corresponding Euclidean space $\Re^n$, and x is given data set for one situation. Thus, from (5), the margins can be described as follows:

for all situations above hyperplane

$$\overrightarrow{\omega}\,\overrightarrow{x} - b = -1 \tag{6}$$

for all situations below hyperplane

$$\overrightarrow{\omega}\,\overrightarrow{x} - b = 1 \tag{7}$$

if $x = x_1, x_2, x_3, ..., x_n$, then the distance from x to hyperplane is:

$$k = \frac{\overrightarrow{x}\,\overrightarrow{\omega} - b}{\sqrt{\omega^2}} \tag{8}$$

and in Cartesian form, we have

$$\mid k \mid = \frac{\mid \omega_1 x_1 + \omega_2 x_2 + ... + \omega_n x_n \mid}{\mid \omega \mid} \tag{9}$$

In our case, $n = 8$. So, we have

$$\mid k \mid = \frac{\mid \omega_1 x_1 + \omega_2 x_2 + ... + \omega_8 x_8 \mid}{\sqrt{\omega_1^2 + \omega_2^2 + ... + \omega_8^2}} \tag{10}$$

This equation can be solved in different ways; one of them is optimization where ω and b are searched as subject to:

$$y_i(\overleftarrow{\omega}\,\overrightarrow{x_i} - b) \geq 1; i = 1, 2, ..., 8 \tag{11}$$

The Optimization calculations are conducted via software tool for all 7 signals according to training data stack. In this way, using heuristic algorithms are useful [61]–[63]. After training, the output training results for all 7 signals are presented in Table VI. Note that:

- 0:0 - 8 means 8 recorded cases in testing situations of not Observed and not predicted,
- 0:1 - 1 means 1 recorded case of testing situation where not observed and predicted situation,
- 1:0 - 0 means 0 recorded case of testing situation where observed and not predicted situation, and
- 1:1 - 45 means 45 recorded cases where is observed and predicted present

The data feed for particular SVM algorithm and its positioning is depicted in Fig. 11.

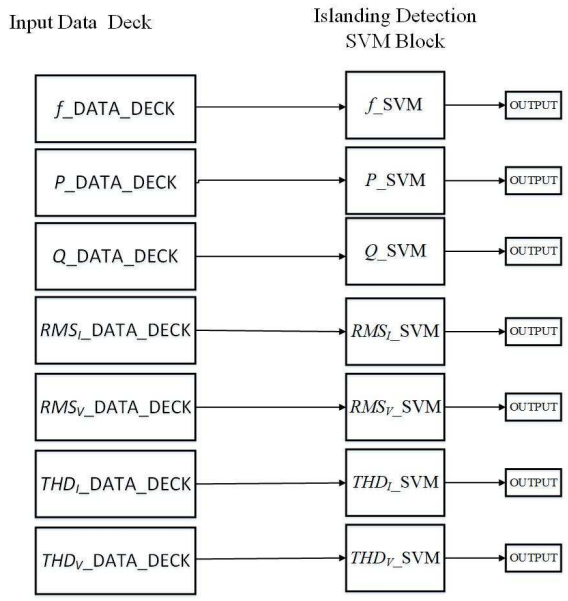

Fig. 11. Data set to feed SVM classification module for islanding detection.

Also, for better illustration of the mentioned concepts, Fig. 12 shows the behavior of RMS_I, RMS_U, THD_i, THD_U, P, Q and f, after islanding. There is no huge difference between those two sets, therefore, we need to discriminate two sets of data for islanding and PHEV rapid charging. The SVM is trained as a two-part system so that one part detects islanding phenomenon and other detect PHEV rapid charging. So, when islanding detection module detects the islanding and PHEV rapid charging detection module does not, then there is a islanding scenario, and otherwise, PHEV rapid charging is occurred. The signals shown in Fig. 12 clearly show that

TABLE VI
OUTPUT TRAINING DETAILS FOR SVM ISLANDING DETECTION

Item	Islanding Training Results						
	f	P	Q	RMS_I	RMS_V	THD_I	THD_V
Kernel function	Gaussian	Cubic	Gaussian	Cubic	Cubic	Cubic	Cubic
Kernel scale	0.71	1	2.8	0.38	0.71	2.26	1.68
Number of observations (Observed vs Predicted: 0:0, 0:1, 1:0, 1:1)	8,1,0,45	6,3,0,45	3,6,0,45	4,5,1,44	2,7,0,45	9,0,1,44	8,1,0,45
Efficiency (Observed / Predicted)	0.99	0.89	0.86	0.93	0.74	0.98	0.91
Principal Component Analysis (95 %)	Yes	Yes	Yes	Yes	Yes	Yes	Yes

they are parts of same sets of anomaly and therefore, the same SVM-based discrimination method between islanding and PHEV rapid charging is used. It should be further noted that different kernel functions are used for same signal and for reactive energy (Q) and moreover, the same kernel with different kernel scale makes SVM Gramian matrix smaller due to the higher training data dispersion.

C. UL1741 Test Conditions

For testing the study system, UL1741 standard is used which describes the conditions for anti-islanding protection of DG units. In the description delegated by UL1741 standard, the active and reactive power load is adjusted to DG in 25%, 50%, 100% and 125% of the nominal generated power of PV system. The reactive power is further adjusted between -5% and +5% of rated active power in 1% steps. In order to test the proposed method under UL1741 standard conditions for system shown in Figs. 1 and 2. Five simulation scenarios are considered:

1) $Scenario1$: Active power load is 100% of generated power, reactive power of load is 0%, power factor is 1.
2) $Scenario2$: Active power load is 50% of generated power, reactive power of load is 0%, power factor is 1.
3) $Scenario3$: Active power load is 125% of generated power, reactive power of load is 0%, power factor is 1.
4) $Scenario4$: Active power load is 100% of generated power, reactive power of load is -1%, power factor is negative.
5) $Scenario5$: Active power load is 50% of generated power, reactive power of load is 1%, power factor is positive.

The RLC load for mentioned scenarios are presented in Table VII. Also, the above-mentioned scenarios are considered less than three different load conditions regarding generated power namely 2%, 100% and 200% of the generated power. Additional testing conditions are involved based on UL1741 standard for different quality factor (QF) values shown by Q. The testing conditions for different values of QF are also prepared based on UL1741 standard. The RLC load for different QF values is presented in Table VIII. The different RLC values are considered less than three different load conditions regarding generated power: 2%, 100% and 200% of nominal PV generation power. After UL1741 standard test, the model is tested for two different PHEV charging scenarios. The first scenario is situation where PHEV rapid charging event is occurred at 0.1 sec. followed by no islanding event.

TABLE VII
RLC LOAD CONFIGURATION FOR TESTING SCENARIOS UNDER UL1741 STANDARD.

Scenario	P [%]	Q [%]	R [Ω]	L [H]	C [F]
1	100%	100%	0.011561	0.00345	0.002037
2	50%	100%	0.023121	0.00345	0.002037
3	125%	100%	0.009249	0.00345	0.002037
4	100%	99%	0.011561	0.003488	0.,002037
5	100%	101%	0.011561	0.003419	0.002037

TABLE VIII
RLC LOAD ACCORDING TO DIFFERENT VALUES OF QF.

Scenario	Q	R [Ω]	L [H]	C [F]
1	1.003	2.304	0.00607	0.00115
2	2.008	2.304	0.00304	0.00231
3	2.503	2.304	0.00244	0.00288
4	3.008	2.304	0.00203	0.00346
5	4.012	2.304	0.00152	0.00461
6	5.002	2.304	0.00122	0.00575

The second scenario is when PHEV rapid charging at 0.1 sec. followed by islanding event at 0.2 sec. The reason for this test comes from technical properties of PHEV rapid charging which can almost bring DG in short circuit, because the inner resistance of hybrid and/or electric car is so small that DC the current going into the car's battery is huge. This event is detected by the IED at the PCC as a heavy consumer interconnection, or short circuit, if rapid charging of PHEV is not softly started.

The RLC load parameters are according to the cases presented in Table VII, for different Qf values mentioned in Table VIII, and two scenarios for rapid PHEV charging presented in Table IX.

IV. SIMULATION RESULTS

The testing model for simulating the proposed SVM-based anti-islanding protection strategy is made according to real-life study system described in Section II. Fig 2 illustrates the study system with one DG with corresponding parameters presented in Table X and Table XI. There are three CBs installed in the DN: the first one for islanding conditions, the second one

TABLE IX
PHEV RAPID CHARGING TEST SCENARIOS.

	Scenario	Time
1	Rapid charging - yes	0.1 sec.
	Islanding- no	–
2	Rapid charging - yes	0.1 sec.
	Islanding- yes	0.2 sec.

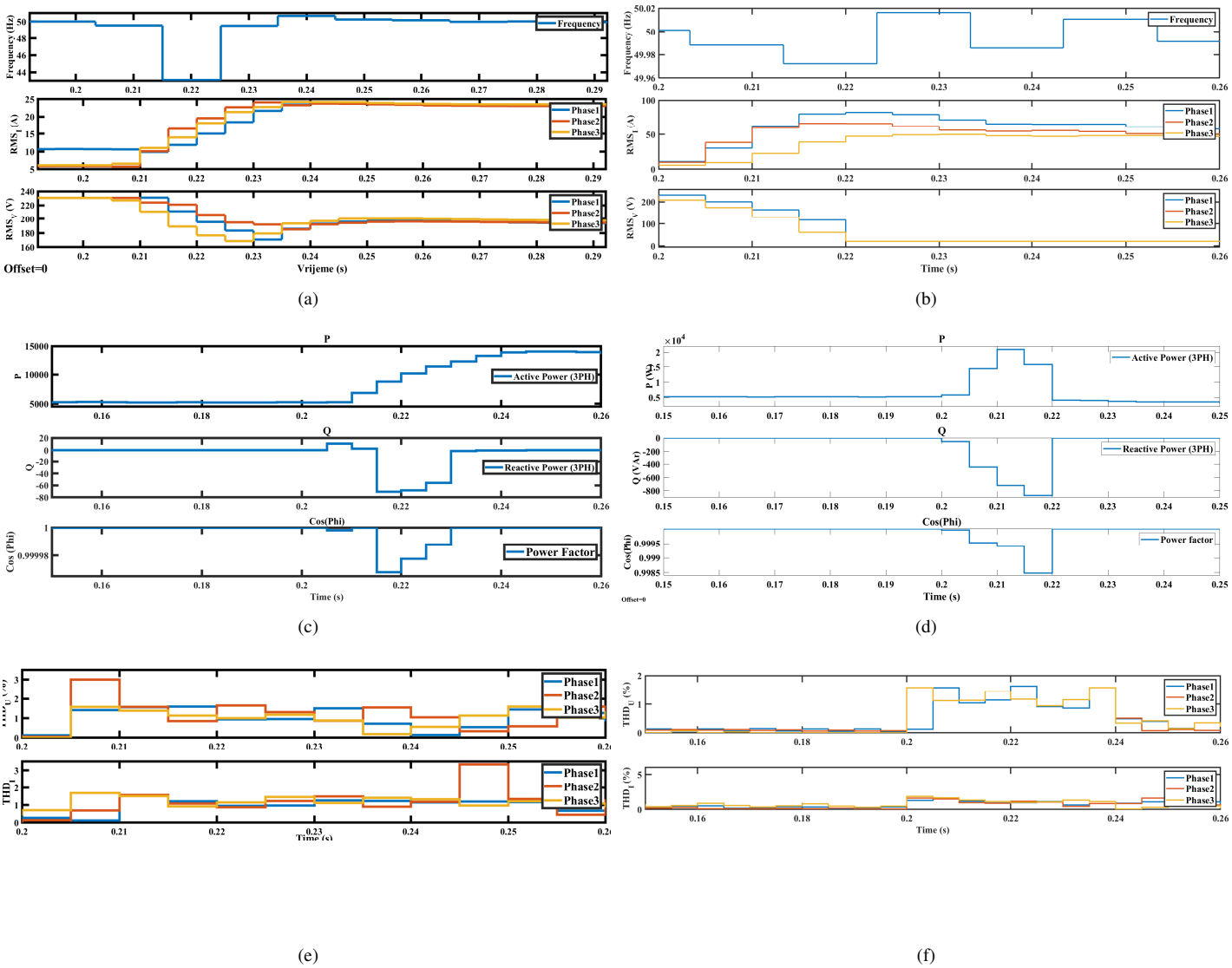

Fig. 12. The behavior of grid signals after islanding and PHEV rapid charging: (a) RMS_I, RMS_U, and f after islanding, (b) RMS_I, RMS_U, and f after PHEV rapid charging, (c) P, Q and Power Factor after islanding, (d) P, Q and Power Factor after PHEV rapid charging, (e) THD_i and THD_U after islanding, and (f) THD_i and THD_U after PHEV rapid charging.

for DG separation from grid, and the third one for injecting additional RLC load. In all of the tests, islanding is occurred at 0.2 sec. In order to confirm islanding, the signal must switch from *on-syn.* stage to *off-isl.* stage.

The testing is conducted based on five scenarios which are all conducted in separated tests and reports: more than one DG in the grid, additional load injection, UL1741 test conditions, PHEV rapid charging and comparison with other reported methods.

A. Case 1: Multiple Distributed Generators

In this subsection, the presented results are obtained from testing scenario of two DGs work in the same grid at the same PCC, as depicted in Fig. 13. The PV panel specification are created according to Table II. The obtained results are presented in Fig 14 and Table XII. Based on the presented results, the SVM successfully detects islanding when parallel DGs are connected to the same PCC.

TABLE X
SIMULATION MODEL PARAMETERS

DG power	21 kW
Inverter input DC voltage	300-310 V
PCC voltage (L-L)	390-400 V
Nominal frequency	50 Hz
DN resistance	0.89 Ω
DN inductance	0.016 H
DG current filter inductance	0.01 H
DG voltage filter capacitance	12 kF

B. Additional Load Injection

The next study deals with testing of the study system scenario with additional load injection into LV DN. The obtained results are provided in Fig. 15 and Table XIII. An amount of 10 kW additional load is injected at the same PCC. Based on the presented results, it is clear that there is no tripping in SVM-based islanding detection block. With simple

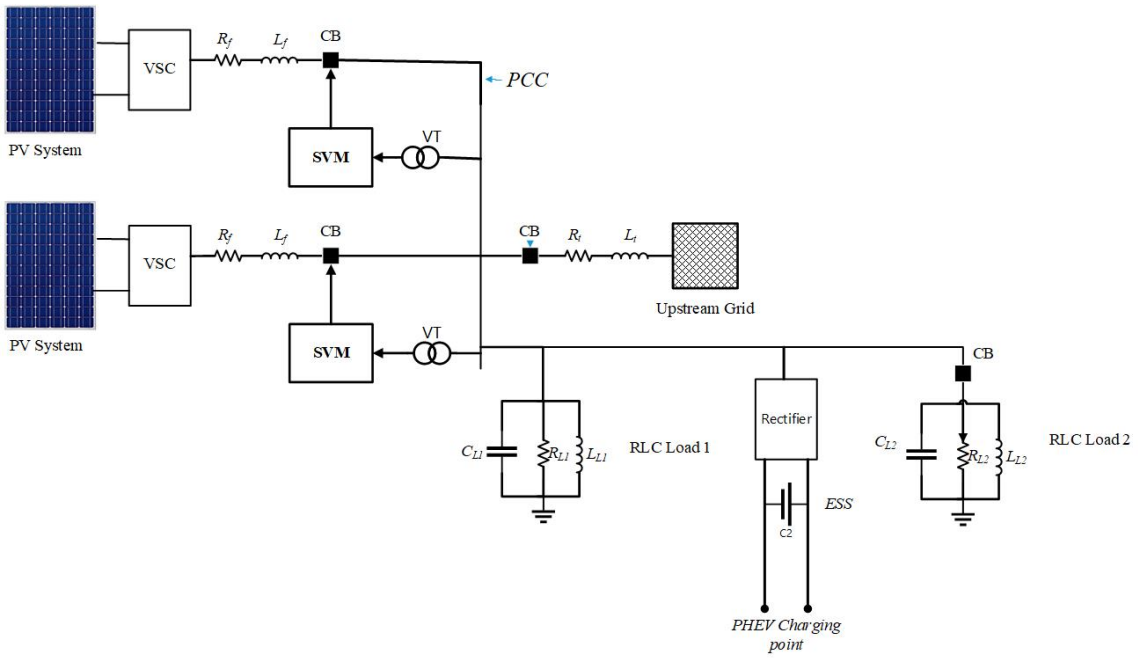

Fig. 13. Single line diagram for Multi-DG system with DN, load and EES based on real-life example.

TABLE XI
DG UNIT (PV SYSTEM) PARAMETERS

Modules type	Soltech 1STH-215-P
Maximum power	213.15 W
Voltage at MPP	29 V
Current at MPP	7.35 A
Short circuit current	7.84 A
Open circuit voltage	36.3 V
Maximum system voltage	360 V
Module number	11x11

TABLE XII
MULTIPLE DG UNITS CASE: OUTPUTS OF THE PROPOSED SVM-BASED ANTI-ISLANDING DETECTION STRATEGY.

	SVM-based Islanding Detection	
	Output	Detection time from event [ms]
f	TRUE	25
P	TRUE	40
Q	TRUE	0
RMS_I	TRUE	40
RMS_V	TRUE	0
THD_I	TRUE	30
THD_V	TRUE	0

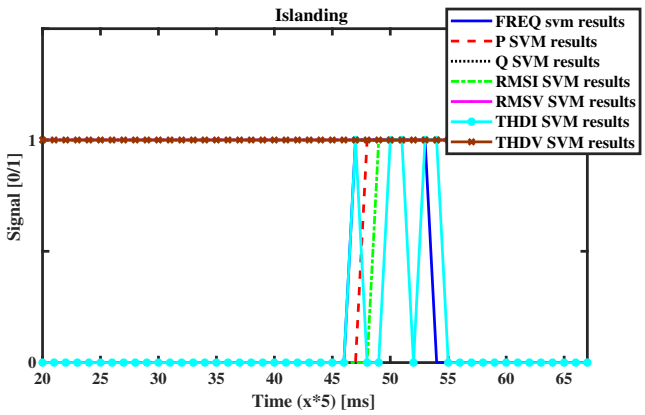

Fig. 14. Multiple DG units case: simulation of the resulted signals for the proposed SVM-based anti-islanding protection strategy.

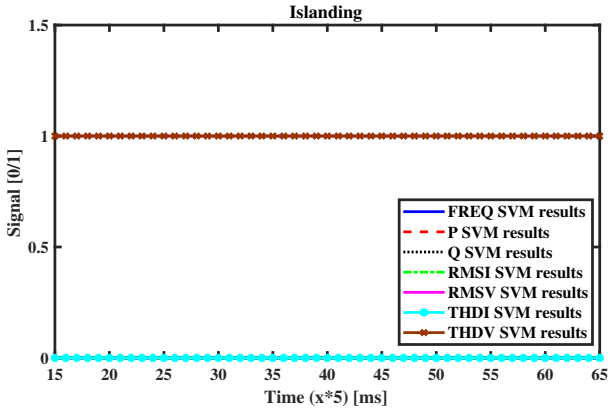

Fig. 15. Additional load injection case: simulation of the resulted signals for the proposed SVM-based anti-islanding protection strategy.

linear transformation, *FALSE* can be converted to *TRUE* but the detection time is left out because there is no tripping, and therefore, there is no islanding event.

C. Method Testing under UL1741 Conditions

In this part of the analysis, for the sake of evaluating the proposed method under UL1741 standard conditions, the results are presented based on the testing conditions mentioned in Table VII and Table VIII, and the results are presented in

TABLE XIII
ADDITIONAL LOAD INJECTION CASE: OUTPUTS OF THE PROPOSED SVM-BASED ANTI-ISLANDING DETECTION STRATEGY

	SVM-based Islanding Detection	
	Output	Detection time from event
f	FALSE	-
P	FALSE	-
Q	FALSE	-
RMS_I	FALSE	-
RMS_V	FALSE	-
THD_I	FALSE	-
THD_V	TRUE	-

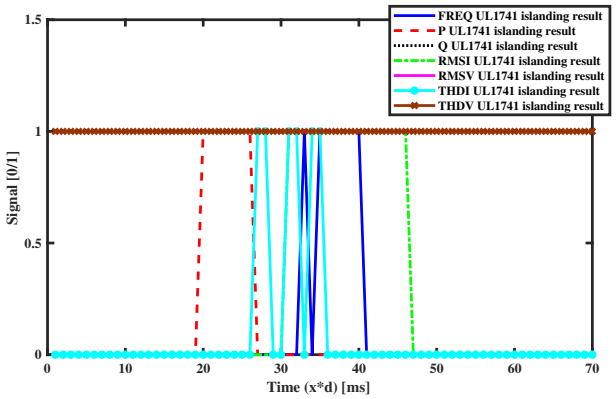

Fig. 16. UL1741 standard test case: simulation of the resulted output signals from SVM based on the parameters of Table VII.

Fig. 16 and Fig 17 and Table XIV. As mentioned, the output signal is formed in lines and processed by SVMs to produce the output. The islanding occurs at 0.2 sec. from the beginning of the timeline. From one number to another number, the time gap is 5 msec. According to Fig. 16 and Fig. 17, islanding occurs in 0.1 sec. and is detected by all signals within 45-60 msec., later. The output signals are used for anti-islanding protection and it is obvious that all 7 signals change their state after islanding event. According to the output data, islanding detection is achieved in scenario of UL1741 standard.

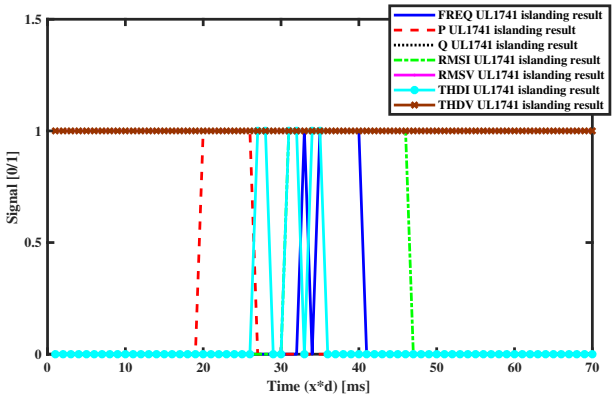

Fig. 17. UL1741 standard test case: simulation of the resulted output signals from SVM based on the parameters of Table VIII.

TABLE XIV
OUTPUT VALUES ACCORDING TO FIG. 16 AND FIG. 17.

Case	Fig. 16	Fig. 17
CASE 1	50 msec.	55 msec.
CASE 2	50 msec.	55 msec.
CASE 3	50 msec.	55 msec.
CASE 4	50 msec.	55 msec.
CASE 5	50 msec.	55 msec.
CASE 6	-	55 msec.

D. PHEV Rapid Charging with/without Islanding

First, we study the situation that the PHEV rapid charging occurs and islanding does not happen. The impact of the PHEV rapid charging is studied using parameters presented in Table I. As mentioned, the PHEV rapid charging demands huge power from the charging station due to its small resistance at the charging moment when the PHEV is connected to the BESS, with constant connection to the LV-DN at the rectifier AC side, and constant connection of rectifier DC side to the ESS, as shown in Fig. 2. Based on the single line diagram (SLD) shown in Fig. 2, rapid charging makes similar effect on LV-DN as high load switching is happened with low inner resistance. The effects of rapid charging are presented on Figs. 18 and 19 and the SVM results are presented in Fig. 20. There is a rapid charging scenario and half full ESS in micro grid, not in electric car. Fig. 19 depicts ESS in microgrid, not in electric vehicle. The battery bank in the BESS is at 50 % state of charge (SoC) and it will be recharged until PHEV connects and starts its rapid charging regime. As shown on Fig. 20, the rapid charging moment begins at t = 0.135 sec. and the SVM does not generate the islanding signal at rapid charging mode.

As mentioned before, the PHEV rapid charging inflicts a huge power-flow from charging station due to its small resistance at the charging moment, when the PHEV is connected to the BESS with a constant connection to the LV-DN at the rectifier AC side, and is constantly connected to the DC side of the rectifier in PV plant. The BESS is at 50% state of charge (SoC) and it will be recharging until PHEV connects and starts its rapid charging regime. The rapid charging moment begins at t = 0.135 sec. and the SVM does not generate the islanding signal at rapid charging mode. In the next scenario, the islanding occurs after rapid charging so that both events are combined. At t = 100 msec., the rapid charging is done and at t = 200 msec., the islanding occurs. The results are presented in Figs. 21 and 22. From 21, it can be observed that the output islanding signal is not triggered after rapid charging. There is a different situation which is shown in Fig. 22 where the rapid charging moment is followed by islanding (t = 200 msec.), and the SVM signals are generated only when islanding occurs (not in PEHV rapid charging) which makes the SVM to be a selective islanding detection method.

E. Analysis of Non-Detection Zone

Discovering NDZ area indicates usage of at-least two different parameters which may or not be related in measuring manner speaking. In this case, we take RMS_V and P (generated power from DG) in the range of 0.9-1.1 p.u. for $RMSV$

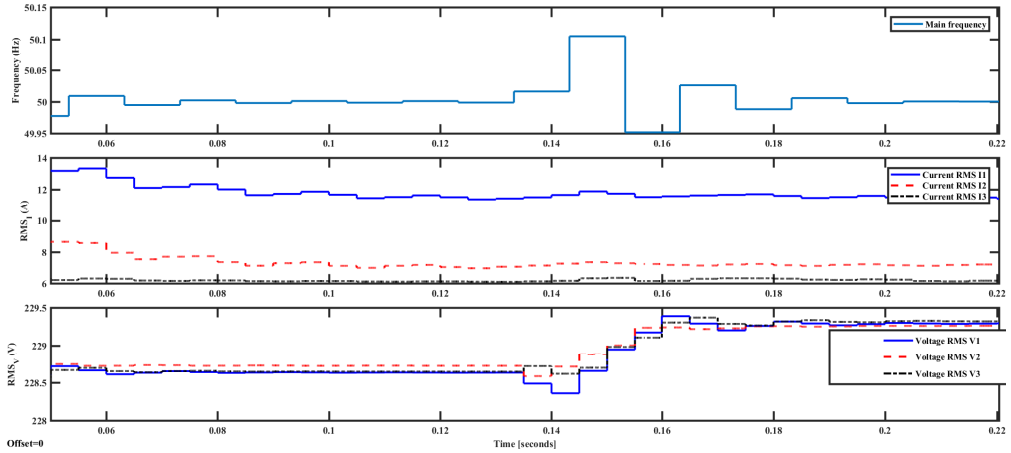

Fig. 18. Effect of PHEV rapid charging on LV-DN in PCC.

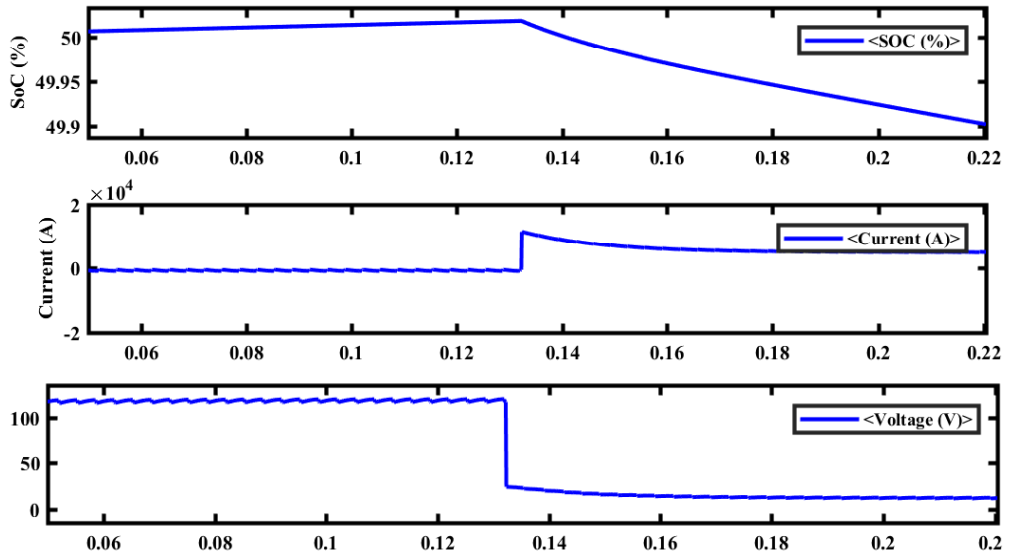

Fig. 19. Trend of ESS response in PHEV rapid charging at rectifier DC side.

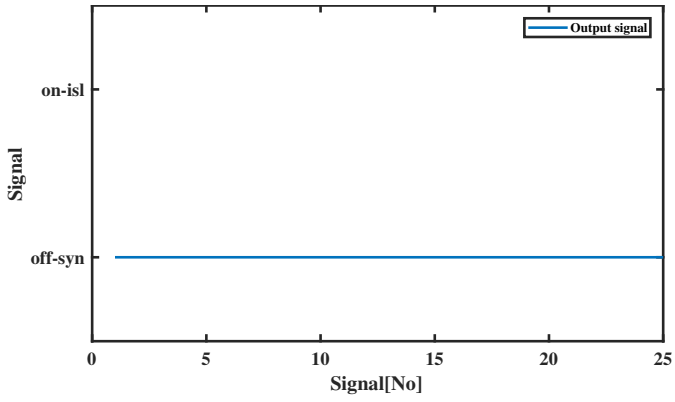

Fig. 20. SVM output results for rapid charging scenario

.

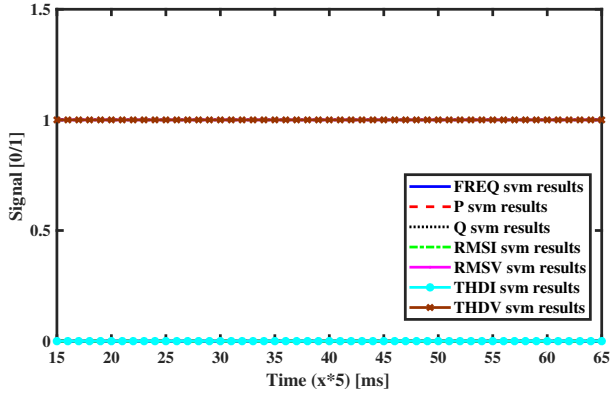

Fig. 21. PHEV rapid charging case without islanding event: simulation of the resulted signals for the proposed SVM-based anti-islanding protection.

with steps of 0.01, and 0.05-1.15 p.u. for P with steps of 0.05. The results are presented in Table XV with red marked cells

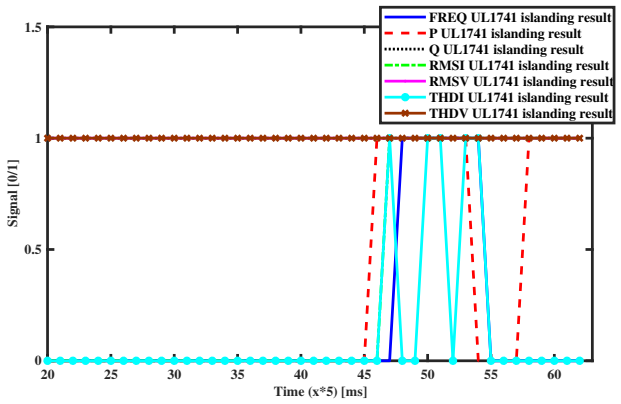

Fig. 22. PHEV rapid charging case with islanding event: simulation of the resulted signals for the proposed SVM-based anti-islanding protection.

where the islanding is not detected, and white ones where the islanding is detected.

Fig. 23 shows detection time for every testing situation which NDZ is field, and presents NDZ using those 2 parameters and detection time in all testing cases of p.u. of both parameters (taking the range of 0-23 kW for P with steps of 0.01, and 358-437 volt for RMS_V with steps of 0.05). The simulation studies indicate that the best results are obtained when the generated power is equal or higher than the nominal installed power in DG and RMS_V is around 1 p.u. or higher. This is due to the input values for SVM data training set which are collected when RMS_V and P are almost around full generation capacity of DG and nominal voltage of distribution grid.

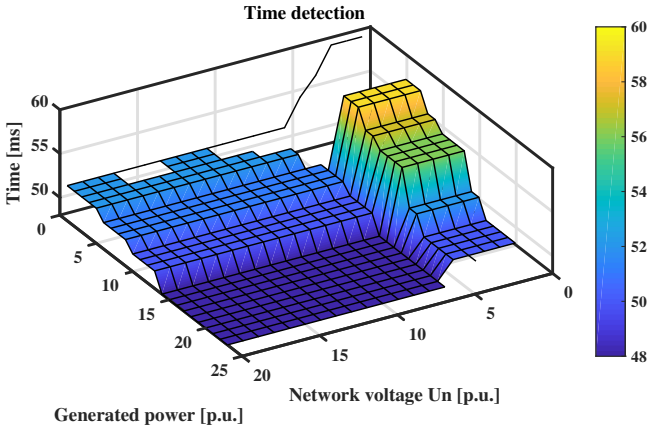

Fig. 23. Detection time disposition.

F. Comparison with Other Similar Techniques

Based on the nature of SVM, we selected some of the related previously-reporte islanding detection methods from [4], [60], [64]–[66] for comparison (Table XVI). The categories of this comparison are detection time, accuracy and NDZ. The detection time of the proposed method is compared with detection time of other reported techniques from published papers. Detection time is read from reference papers and the accuracy and the NDZ are calculated based on (12) and (13) as:

$$I_{ocu} = 100 - \frac{100}{N_M} + N_M \tag{12}$$

$$I_{NDZ} = N_{act} \times A_M + (N_{pas})^{P_M} \tag{13}$$

where, A_M is equal to 5and P_M is 2. The comparative results prove the capability of the proposed SVM-based strategy to be fit for anti-islanding protection and further as a technique for discrimination between islanding and PHEV rapid charging (Table XVI and Fig. 24). Besides the presented comparison categories, some other parameters can be taken into consideration, including but not limited to: time for method training, number of monitored signals, number of samples, measurement costs, etc.

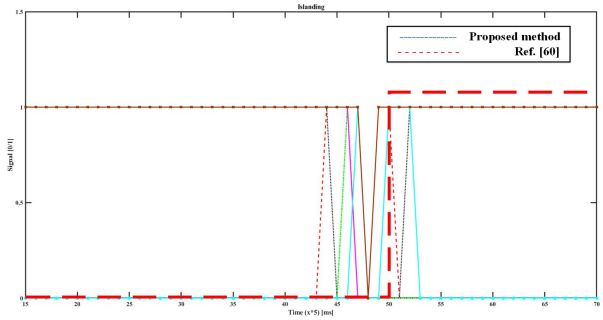

Fig. 24. Comparison of the proposed SVM-based strategy against Ref. [60].

V. Conclusion

This paper investigated the classification capability of support vector machines to protect a PV-based LV active distribution network from anti-islanding and its discrimination from PHEV rapid charging. In this study, we used seven signals for detecting the islanding phenomenon namely frequency, active power, reactive power, and THD and RMS values of voltage current signals. These signal were used as training and testing polygon for the proposed SVM-based algorithm. The proposed method learned dips and swells of the involved signals at the event occasion. We verified the performance of the proposed strategy based on digital time-domain simulation studies conducted in MATLAB/Simulink software environment using the model of a real-life practical PV-based microgrid located in Jajce, Bosnia-Herzegovina. The SVM modules were trained based on a data set including samples of the related signals which were experimentally measured by using a fast high-frequency custom-made IED used as an on-site measurement device. Due to passive nature of the proposed method, the energy quality and other protection measurements were not affected by detecting procedure. We addressed the sensitivity and discrimination capability of the proposed SVM-based anti-islanding strategy and its sensitiveness by involving PHEV rapid charging scenario. The obtained results revealed that the proposed method can successfully detect the islanding

TABLE XV
ISLANDING DETECTION SCENARIOS BASED ON VOLTAGE (IN P.U.) ACQUIRED FROM DISTRIBUTION NETWORK AND GENERATED POWER OF DG.

ISLANDING DETECTION																					
		Distribution Network voltage																			
	[p.u.]	0.9	0.91	0.92	0.93	0.94	0.95	0.96	0.97	0.98	0.99	1	1.01	1.02	1.03	1.04	1.05	1.06	1.07	1.08	1.09
Generated Active Power	0.05	60	60	60	57	55	52	52	52	52	52	52	52	52	52	52	52	52	52	52	52
	0.1											52	52	52	52			52	52	52	52
	0.15									52	52	52	52	52	52	52	52	52	52	52	52
	0.2							52	52	52	52	52	52	52	52	52	52	52	52	52	52
	0.25							52	52	52	52	52	52	52	52	52	52	52	52	52	52
	0.3						51	51	51	51	51	51	51	51	51	51	51	51	51	51	51
	0.35	59	59	59	59	59	51	51	51	51	51	51	51	51	51	51	51	51	51	51	51
	0.4	59	59	59	59	59	51	51	51	51	51	51	51	51	51	51	51	51	51	51	51
	0.45	59	59	59	59	59	51	51	51	51	51	51	51	51	51	51	51	51	51	51	51
	0.5	57	57	57	57	57	50	50	50	50	50	50	50	50	50	50	50	50	50	50	50
	0.55	57	57	57	57	57	50	50	50	50	50	50	50	50	50	50	50	50	50	50	50
	0.6	56	56	56	56	56	50	50	50	50	50	50	50	50	50	50	50	50	50	50	50
	0.65	56	56	56	56	56	50	50	50	50	50	50	50	50	50	50	50	50	50	50	50
	0.7	56	56	56	56	56	48	48	48	48	48	48	48	48	48	48	48	48	48	48	48
	0.75	56	56	56	56	56	48	48	48	48	48	48	48	48	48	48	48	48	48	48	48
	0.8	52	52	52	52	52	48	48	48	48	48	48	48	48	48	48	48	48	48	48	48
	0.85	52	52	52	52	52	48	48	48	48	48	48	48	48	48	48	48	48	48	48	48
	0.9	50	50	50	50	50	48	48	48	48	48	48	48	48	48	48	48	48	48	48	48
	0.95	50	50	50	50	50	48	48	48	48	48	48	48	48	48	48	48	48	48	48	48
	1	50	50	50	50	50	48	48	48	48	48	48	48	48	48	48	48	48	48	48	48
	1.05	50	50	50	50	50	48	48	48	48	48	48	48	48	48	48	48	48	48	48	48
	1.1	50	50	50	50	50	48	48	48	48	48	48	48	48	48	48	48	48	48	48	48
	1.15				50		48	48	48	48	48	48	48	48	48	48	48	48	48	48	48

TABLE XVI
THE COMPARATIVE RESULTS.

	Detection time [s]	Accuracy[%]	NDZ
Ref. [64]	0.270	2	1 %
Ref. [65]	0.200	2	1 %
Ref. [66]	0.050	2	1 %
Ref. [4]	0.040	78.71	49 %
Ref. [60]	0.050	99.49	9.89 %
The proposed method	0.040	100.00	9.52 %

phenomenon with a high level of accuracy, and can properly discriminate it with PHEV rapid charging. The extension of the proposed strategy for islanding and grid-fault detection and discrimination is the subject of the future research of the authors.

REFERENCES

[1] *IEEE Standard on Interconnecting Distributed Resources with Electric Power Systems,*, IEEE Std. 1547, 2003.

[2] S. Nikolovski, H. R. Baghaee, and D. Mlakic, "Islanding detection of synchronous generator-based DGs using rate of change of reactive power," *IEEE Systems Journal*, vol. PP, no. 99, pp. 1–11, Jan. 2019.

[3] K. Sareen, B. R. Bhalja, and R. P. Maheshwari, "A hybrid multi-feature based islanding detection technique for grid connected distributed generation," *Int. Journal of Emerging Electric Power Systems*, vol. 18, no. 1, pp. 1–16, jan 2017.

[4] D. Mlakic, H. R. Baghaee, and S. Nikolovski, "A novel ANFIS-based islanding detection for inverter–interfaced microgrids," *IEEE Trans. on Smart Grid*, vol. PP, no. 99, pp. 1–13, 2018.

[5] F. Bignucolo, A. Raciti, and R. Caldon, "Coordinating active and reactive energy balances in islanded networks supported by renewables and BESS," in *3rd Renewable Power Generation Conf. (RPG 2014)*. Naples, Italy: Institution of Engineering and Technology, Sep. 2014, pp. 1–6.

[6] M. Khodaparastan, H. Vahedi, F. Khazaeli, and H. Oraee, "A novel hybrid islanding detection method for inverter-based DGs using SFS and ROCOF," *IEEE Trans. on Power Delivery*, vol. 32, no. 5, pp. 2162–2170, oct 2017.

[7] H. Zeineldin and S. Kennedy, "Sandia frequency-shift parameter selection to eliminate nondetection zones," *IEEE Trans. on Power Delivery*, vol. 24, no. 1, pp. 486–487, jan 2009.

[8] H. Vahedi, M. Karrari, and G. B. Gharehpetian, "Accurate SFS parameter design criterion for inverter-based distributed generation," *IEEE Trans. on Power Delivery*, vol. 31, no. 3, pp. 1050–1059, jun 2016.

[9] D. Voglitsis, N. P. Papanikolaou, and A. C. Kyritsis, "Active cross-correlation anti-islanding scheme for PV module integrated converters in the prospect of high penetration levels and weak grid conditions," *IEEE Trans. on Power Electronics*, pp. 1–1, 2018.

[10] D. Voglitsis, N. Papanikolaou, and A. C. Kyritsis, "Incorporation of harmonic injection in an interleaved flyback inverter for the implementation of an active anti-islanding technique," *IEEE Trans. on Power Electronics*, vol. 32, no. 11, pp. 8526–8543, nov 2017.

[11] A. S. Subhadra, P. Reddy, and S. . B. Modi, "Islanding detection in a distribution system with modified DG interface controller," *Int. Journal of Applied Power Engineering (IJAPE)*, vol. 6, no. 3, pp. 135–143, dec 2017.

[12] B. Wen, D. Boroyevich, R. Burgos, Z. Shen, and P. Mattavelli, "Impedance-based analysis of active frequency drift islanding detection for grid-tied inverter system," *IEEE Trans. on Industry Applications*, vol. 52, no. 1, pp. 332–341, jan 2016.

[13] A. Yafaoui, B. Wu, and S. Kouro, "Improved active frequency drift anti-islanding detection method for grid connected photovoltaic systems," *IEEE Trans. on Power Electronics*, vol. 27, no. 5, pp. 2367–2375, may 2012.

[14] M. A. Hosani, Z. Qu, and H. H. Zeineldin, "Scheduled perturbation to reduce nondetection zone for low gain sandia frequency shift method," *IEEE Trans. on Smart Grid*, vol. 6, no. 6, pp. 3095–3103, nov 2015.

[15] H. H. Zeineldin and M. M. A. Salama, "Impact of load frequency dependence on the NDZ and performance of the SFS islanding detection method," *IEEE Trans. on Industrial Electronics*, vol. 58, no. 1, pp. 139–146, jan 2011.

[16] H. Vahedi and M. Karrari, "Adaptive fuzzy sandia frequency-shift method for islanding protection of inverter-based distributed generation," *IEEE Trans. on Power Delivery*, vol. 28, no. 1, pp. 84–92, jan 2013.

[17] G.-K. Hung, C.-C. Chang, and C.-L. Chen, "Automatic phase-shift method for islanding detection of grid-connected photovoltaic inverters," *IEEE Trans. on Energy Conversion*, vol. 18, no. 1, pp. 169–173, mar 2003.

[18] S. Yuyama, T. Ichinose, K. Kimoto, T. Itami, T. Ambo, C. Okado, K. Nakajima, S. Hojo, H. Shinohara, and S. Ioka, "A high speed frequency shift method as a protection for islanding phenomena of utility interactive PV systems," *Solar Energy Materials and Solar Cells*, vol. 35, pp. 477–486, sep 1994.

[19] M. Trabelsi and H. Abu-Rub, "A unique active anti-islanding protection for a quasi-z-source based power conditioning system," in *2015 IEEE Applied Power Electronics Conf. and Exposition (APEC)*. Charlotte, NC, USA: IEEE, mar 2015, pp. 2237–2243.

[20] N. Liu, C. Diduch, L. Chang, and J. Su, "A reference impedance-based passive islanding detection method for inverter-based distributed generation system," *IEEE Journal of Emerging and Selected Topics in Power Electronics*, vol. 3, no. 4, pp. 1205–1217, dec 2015.

[21] S. Murugesan and V. Murali, "HYBRID ANALYSING TECHNIQUE BASED ACTIVE ISLANDING DETECTION FOR MULTIPLE DGs," *IEEE Trans. on Industrial Informatics*, vol. PP, no. 99, pp. 1–10, Jun. 2018.

[22] S. Murugesan, V. Murali, and S. A. Daniel, "Hybrid analyzing technique for active islanding detection based on d-axis current injection," *IEEE Systems Journal*, vol. PP, no. 99, pp. 1–10, Aug. 2017.

[23] P. Gupta, R. S. Bhatia, and D. K. Jain, "Active ROCOF relay for islanding detection," *IEEE Trans. on Power Delivery*, vol. 32, no. 1, pp. 420–429, feb 2017.

[24] D. Reigosa, F. Briz, C. B. Charro, P. Garcia, and J. M. Guerrero, "Active islanding detection using high-frequency signal injection," *IEEE Trans. on Industry Applications*, vol. 48, no. 5, pp. 1588–1597, sep 2012.

[25] D. D. Reigosa, F. Briz, C. B. Charro, and J. M. Guerrero, "Passive islanding detection using inverter nonlinear effects," *IEEE Trans. on Power Electronics*, vol. 32, no. 11, pp. 8434–8445, nov 2017.

[26] K. Jia, H. Wei, T. Bi, D. W. P. Thomas, and M. Sumner, "An islanding detection method for multi-DG systems based on high-frequency impedance estimation," *IEEE Trans. on Sustainable Energy*, vol. 8, no. 1, pp. 74–83, jan 2017.

[27] D. D. Reigosa, F. Briz, C. B. Charro, and J. M. Guerrero, "Islanding detection in three-phase and single-phase systems using pulsating high-frequency signal injection," *IEEE Trans. on Power Electronics*, vol. 30, no. 12, pp. 6672–6683, dec 2015.

[28] F. Briz, D. Diaz-Reigosa, C. Blanco, and J. M. Guerrero, "Coordinated operation of parallel-connected inverters for active islanding detection using high-frequency signal injection," *IEEE Trans. on Industry Applications*, vol. 50, no. 5, pp. 3476–3484, sep 2014.

[29] D. Reigosa, F. Briz, C. Blanco, P. Garcia, and J. M. Guerrero, "Active islanding detection for multiple parallel-connected inverter-based distributed generators using high-frequency signal injection," *IEEE Trans. on Power Electronics*, vol. 29, no. 3, pp. 1192–1199, mar 2014.

[30] C. Jeraputra and P. Enjeti, "Development of a robust anti-islanding algorithm for utility interconnection of distributed fuel cell powered generation," *IEEE Trans. on Power Electronics*, vol. 19, no. 5, pp. 1163–1170, sep 2004.

[31] Y. Zhu, D. Xu, N. He, J. Ma, J. Zhang, Y. Zhang, G. Shen, and C. Hu, "A novel RPV (reactive-power-variation) antiislanding method based on adapted reactive power perturbation," *IEEE Trans. on Power Electronics*, vol. 28, no. 11, pp. 4998–5012, nov 2013.

[32] X. Chen and Y. Li, "An islanding detection algorithm for inverter-based distributed generation based on reactive power control," *IEEE Trans. on Power Electronics*, vol. 29, no. 9, pp. 4672–4683, sep 2014.

[33] ——, "An islanding detection method for inverter-based distributed generators based on the reactive power disturbance," *IEEE Trans. on Power Electronics*, vol. 31, no. 5, pp. 3559–3574, may 2016.

[34] J. Zhang, D. Xu, G. Shen, Y. Zhu, N. He, and J. Ma, "An improved islanding detection method for a grid-connected inverter with intermittent bilateral reactive power variation," *IEEE Trans. on Power Electronics*, vol. 28, no. 1, pp. 268–278, jan 2013.

[35] H. Ding, Y. Wei, X. Wang, J. Yuan, D. Zhang, J. Zhang, X. Li, and H. Qi, "A novel islanding detection based on adaptive active current disturbance," in *2014 IEEE Conf. and Expo Transportation Electrification Asia-Pacific (ITEC Asia-Pacific)*. Beijing, China: IEEE, aug 2014, pp. 1–5.

[36] B.-G. Yu, M. Matsui, and G.-J. Yu, "A correlation-based islanding-detection method using current-magnitude disturbance for PV system," *IEEE Trans. on Industrial Electronics*, vol. 58, no. 7, pp. 2935–2943, jul 2011.

[37] J.-H. Kim, J.-G. Kim, Y.-H. Ji, Y.-C. Jung, and C.-Y. Won, "An islanding detection method for a grid-connected system based on the goertzel algorithm," *IEEE Trans. on Power Electronics*, vol. 26, no. 4, pp. 1049–1055, apr 2011.

[38] W. I. BOWER and M. ROPP, "Evaluation of islanding detection methods for utility-interactive inverters in photovoltaic systems," Int. Energy Agency, Sandia National Laboratories* Photovoltaic Systems Research and Development, Albuquerque, NM, 87185-0753, USA, techreport, nov 2002.

[39] A. M. I. Mohamad and Y. A.-R. I. Mohamed, "Analysis and mitigation of interaction dynamics in active DC distribution systems with positive feedback islanding detection schemes," *IEEE Trans. on Power Electronics*, vol. 33, no. 3, pp. 2751–2773, mar 2018.

[40] Y.-C. Wu, J. Lin, J.-H. Chen, and H. Ming-Yu, "Islanding detection using RT-lab," *MATEC Web of Conf.s*, vol. 256, p. 04005, 2019.

[41] J. W. S. III, R. H. BONN, J. W. GINN, S. GONZALEZ, and G. KERN, "Development and testing of an approach to anti-islanding in utility-interconnected photovoltaic systems," Sandia National Laboratory, Albuquerque, NM, USA,, techreport, aug 2000.

[42] S.-J. Huang and F.-S. Pai, "A new approach to islanding detection of dispersed generators with self-commutated static power converters," *IEEE Trans. on Power Delivery*, vol. 15, no. 2, pp. 500–507, apr 2000.

[43] A. Danandeh, H. Seyedi, and E. Babaei, "Islanding detection using combined algorithm based on rate of change of reactive power and current THD techniques," in *Asia-Pacific Power and Energy Engineering Conf.* Shanghai, China: IEEE, mar 2012, pp. 1–4.

[44] S.-I. Jang and K.-H. Kim, "An islanding detection method for distributed generations using voltage unbalance and total harmonic distortion of current," *IEEE Trans. on Power Delivery*, vol. 19, no. 2, pp. 745–752, apr 2004.

[45] S. Salman, "New loss of mains detection algorithm for embedded generation using rate of change of voltage and changes in power factors," in *7th Int. Conf. on Developments in Power Systems Protection (DPSP 2001)*. New loss of mains detection algorithm for embedded generation using rate of change of voltage and changes in power factors: IEE, 2001, pp. 82–85.

[46] M. Liserre, A. Pigazo, A. Dell'Aquila, and V. Moreno, "An anti-islanding method for single-phase inverters based on a grid voltage sensorless control," *IEEE Trans. on Industrial Electronics*, vol. 53, no. 5, pp. 1418–1426, oct 2006.

[47] A. Samui and S. R. Samantaray, "Assessment of ROCPAD relay for islanding detection in distributed generation," *IEEE Trans. on Smart Grid*, vol. 2, no. 2, pp. 391–398, jun 2011.

[48] H. Vahedi, G. B. Gharehpetian, and M. Karrari, "Application of duffing oscillators for passive islanding detection of inverter-based distributed generation units," *IEEE Trans. on Power Delivery*, vol. 27, no. 4, pp. 1973–1983, oct 2012.

[49] A. Samui and S. R. Samantaray, "Wavelet singular entropy-based islanding detection in distributed generation," *IEEE Trans. on Power Delivery*, vol. 28, no. 1, pp. 411–418, jan 2013.

[50] D. Mlakic, H. R. Baghaee, and S. Nikolovski, "Gibbs phenomenon-based hybrid islanding detection strategy for VSC-based microgrids using frequency shift, THDU and RMSU," *IEEE Trans. on Smart Grid*, vol. PP, no. 99, pp. 1–12, Nov. 2018.

[51] S. R. Samantaray, K. El-Arroudi, G. Joos, and I. Kamwa, "A fuzzy rule-based approach for islanding detection in distributed generation," *IEEE Trans. on Power Delivery*, vol. 25, no. 3, pp. 1427–1433, jul 2010.

[52] Y. Makwana and B. R. Bhalja, "Islanding detection technique based on relevance vector machine," *IET Renewable Power Generation*, vol. 10, no. 10, pp. 1607–1615, nov 2016.

[53] K.-H. Tan and C.-W. Lan, "DG system using PFNN controllers for improving islanding detection and power control," *Energies*, vol. 12, no. 3, p. 506, feb 2019.

[54] C. Haoran, X. Jianyuan, L. Hui, C. Guoqiang, J. Yuanyu, C. Shengwei, and C. Jiangbo, "Islanding detection method of distribution generation system based on logistic regression," *The Journal of Engineering*, vol. 2019, no. 16, pp. 2296–2300, mar 2019.

[55] S. Nikolovski, H. R. Baghaee, and D. Mlakić, "ANFIS-based peak power shaving/curtailment in microgrids including PV units and BESSs," *Energies*, vol. 11, no. 11, p. 2953, Oct. 2018.

[56] A. Arancibia and K. Strunz, "Modeling of an electric vehicle charging station for fast DC charging," in *IEEE Int. Electric Vehicle Conf.* Greenville, SC, USA: IEEE, mar 2012, pp. 1–6.

[57] D. Mlakić, S. N. Nikolovski, and E. Alibašić, "Designing automatic meter reading system using open source hardware and software," *Int. Journal of Electrical and Computer Engineering (IJECE)*, vol. 7, no. 6, pp. 3282–3291, dec 2017.

[58] M. Brenna, M. Longo, and W. Yaïci, "Modelling and simulation of electric vehicle fast charging stations driven by high speed railway systems," *Energies*, vol. 10, no. 9, p. 1268, aug 2017.

[59] T. Dragicevic, S. Sucic, J. C. Vasquez, and J. M. Guerrero, "Flywheel-based distributed bus signalling strategy for the public fast charging station," *IEEE Transactions on Smart Grid*, vol. 5, no. 6, pp. 2825–2835, nov 2014.

[60] B. Matic-Cuka and M. Kezunovic, "Islanding detection for inverter-based distributed generation using support vector machine method," *IEEE Trans. on Smart Grid*, vol. 5, no. 6, pp. 2676–2686, nov 2014.

[61] A. Parizad, H. Baghaee, A. Tavakoli, and S. Jamali, "Optimization of arc models parameter using genetic algorithm," IEEE, Sharjah, United Arab Emirates, pp. 1–7, Nov. 2009.

[62] H. Baghaee, M. Jannati, B. Vahidi, S. Hosseinian, and H. Rastegar, "Improvement of voltage stability and reduce power system losses by optimal GA-based allocation of multi-type FACTS devices," in *2008 11th Int. Conf. on Optimization of Electrical and Electronic Equipment*. Brasov, Romania: IEEE, may 2008, pp. 209–214.

[63] A. K. Kaviani, H. R. Baghaee, and G. H. Riahy, "Optimal sizing of a stand-alone wind/photovoltaic generation unit using particle swarm optimization," *SIMULATION*, vol. 85, no. 2, pp. 89–99, feb 2009.

[64] V. Merlin, R. Santos, A. Grilo, J. Vieira, D. Coury, and M. Oleskovicz, "A new artificial neural network based method for islanding detection of distributed generators," *Int. Journal of Electrical Power & Energy Systems*, vol. 75, pp. 139–151, feb 2016.

[65] N. Ghadimi and B. Sobhani., "Adaptive neuro-fuzzy inference system (anfis) islanding detection based on wind turbine simulator," *Int. J. of Physical Sciences*, vol. 8, no. 27, pp. 1424–1436, Jul. 2013.

[66] N. Ghadimi, "An adaptive neuro-fuzzy inference system for islanding detection in wind turbine as distributed generation," *Complexity*, vol. 21, no. 1, pp. 10–20, apr 2014.

Hamid Reza Baghaee (SM' 2008, M' 2017) received his Ph.D. degree in Electrical Engineering from Amirkabir University of Technology (AUT) in 2017. Since 2007 to 2017, he had been a teaching and research assistant in department of electrical engineering of AUT. He is author of one book, one published chapter book, 40 journal and 50 conference papers and owner of one registered patents. His special fields of interest are micro and smart grids, application of power electronic in power systems, distributed generation and renewable energies, power system operation, and control, and application of artificial intelligence in power systems.

Dr. Baghaee is also the winner of four national and international prizes, as the best dissertation award, from Iranian scientific organization of smart grids (ISOSG) in December 2017, Iranian energy association (IEA) in February 2018, AUT in December 2018, and IEEE Iran Section in May 2019 for his PhD dissertation. He is also reviewer of several IEEE and IET journals and guest editor of several special issues in IEEE Transactions, and IET and MDPI journals, and member of scientific program committees of several IEEE conferences.

Dragan Mlakić (M' 2015) was born in Travnik on June 15, 1981. He obtained his BSc degree (2007) and MSc degree (2013), in electrical engineering at Faculty of Electrical Engineering, University of Sarajevo, Bosnia and Hercegovina. He is also Ph.D. student at Faculty Of Electrical Engineering, Computer Science And Information Technology (FERIT) Osijek , Croatia. Presently he works as Engineer in Electric power company HZ-HB Inc. Mostar, Novi Travnik, Bosnia and Herzegovina and as Assistant Professor at the Software Engineering Department at Faculty of Information Technology, University Vitez, Bosnia and Herzegovina. His main research interests are artificial intelligence, AI safety, renewable energy sources, energy quality, smart grid and power protection.

Srete Nikolovski (M' 1995, SM' 2005) was born in Belgrade on October 1, 1954. He obtained his BSc degree (1978) and MSc degree (1989) in Electrical Engineering at the Faculty of Electrical Engineering, University of Belgrade and his PhD degree (1993) at the Faculty of Electrical and Computing Engineering, University of Zagreb, Croatia. He is a Full Professor at the Department of Power Engineering at the Faculty of Electrical Engineering, Computer Science and Information Technology, University of Osijek, Croatia. His main interests are: Power system reliability, power system protection, integration of distributed generation in power networks, power system modeling and analysis, Arc-flash hazard risk analysis. He had published 46 academic papers in journals and 164 paper in international conferences proceedings. He received from IEEE PES Chapter Outstanding Engineering Award in 2014 for contributions in the field of power system reliability. He is IEEE Senior member of Reliability Society and PES Society.

Tomislav Dragicević (S' 2009, M' 2013, SM' 2017) received the M.Sc. and the industrial Ph.D. degrees in Electrical Engineering from the Faculty of Electrical Engineering, Zagreb, Croatia, in 2009 and 2013, respectively. From 2013 until 2016 he has been a Postdoctoral research associate at Aalborg University, Denmark. From March 2016 he is an Associate Professor at Aalborg University, Denmark where he leads an Advanced Control Lab Advanced Control Lab.

He made a guest professor stay at Nottingham University, UK during spring/summer of 2018. His principal field of interest is design and control of microgrids, and application of advanced modeling and control concepts to power electronic systems. He has authored and co-authored more than 155 technical papers (more than 70 of them are published in international journals, mostly IEEE Transactions) in his domain of interest, 8 book chapters and a book in the field.

He serves as Associate Editor in the IEEE TRANSACTIONS ON INDUSTRIAL ELECTRONICS, in IEEE Emerging and Selected Topics in Power Electronics and in IEEE Industrial Electronics Magazine. Dr. Dragičević is a recipient of the Končar prize for the best industrial PhD thesis in Croatia, and a Robert Mayer Energy Conservation award.